



Measurement of the prompt J/ψ and $\psi(2S)$ polarizations in pp collisions at $\sqrt{s} = 7$ TeV

The CMS Collaboration*

Abstract

The polarizations of prompt J/ψ and $\psi(2S)$ mesons are measured in proton-proton collisions at $\sqrt{s} = 7$ TeV, using a dimuon data sample collected by the CMS experiment at the LHC, corresponding to an integrated luminosity of 4.9 fb^{-1} . The prompt J/ψ and $\psi(2S)$ polarization parameters λ_θ , λ_ϕ , and $\lambda_{\theta\phi}$, as well as the frame-invariant quantity $\tilde{\lambda}$, are measured from the dimuon decay angular distributions in three different polarization frames. The J/ψ results are obtained in the transverse momentum range $14 < p_T < 70$ GeV, in the rapidity intervals $|y| < 0.6$ and $0.6 < |y| < 1.2$. The corresponding $\psi(2S)$ results cover $14 < p_T < 50$ GeV and include a third rapidity bin, $1.2 < |y| < 1.5$. No evidence of large polarizations is seen in these kinematic regions, which extend much beyond those previously explored.

Published in Physics Letters B as doi:10.1016/j.physletb.2013.10.055.

1 Introduction

After considerable experimental and theoretical efforts over the past decades, the understanding of quarkonium production in hadron collisions is still not fully settled [1]. In particular, the polarization of J/ψ mesons is not satisfactorily described in the context of nonrelativistic quantum chromodynamics (NRQCD) [2], where the purely perturbative colour-singlet production [3] is complemented by processes including possible nonperturbative transitions from coloured quark pairs to the observable bound states. The S-wave quarkonia directly produced at high transverse momentum, p_T , are predicted to be transversely polarized [4–6] with respect to the direction of their own momentum. Contrary to this expectation, the CDF Collaboration measured a small longitudinal polarization in prompt J/ψ production [7]. Since the measurement includes both directly produced J/ψ mesons and those resulting from feed-down decays of heavier charmonia, the comparison between the theoretical predictions and the experimental results remained ambiguous [8]. Also the apparent lack of kinematic continuity between the fixed-target and the collider quarkonium polarization data [9] raises doubts on the reliability of these complex measurements. Given the absence of feed-down decays from heavier charmonia affecting $\psi(2S)$ production, the measurements of the $\psi(2S)$ polarization should be particularly informative, especially if made with higher accuracy and extending up to higher p_T than those provided by CDF [7].

The polarization of the $J^{PC} = 1^{--}$ quarkonium states can be measured through the study of the angular distribution of the leptons produced in their $\mu^+\mu^-$ decay [8],

$$W(\cos\vartheta, \varphi|\vec{\lambda}) = \frac{3}{4\pi(3 + \lambda_\vartheta)} (1 + \lambda_\vartheta \cos^2\vartheta + \lambda_\varphi \sin^2\vartheta \cos 2\varphi + \lambda_{\vartheta\varphi} \sin 2\vartheta \cos\varphi), \quad (1)$$

where ϑ and φ are the polar and azimuthal angles, respectively, of the μ^+ with respect to the z axis of the chosen polarization frame. Robust quarkonium polarization measurements require extracting all the angular distribution parameters, $\vec{\lambda} = (\lambda_\vartheta, \lambda_\varphi, \lambda_{\vartheta\varphi})$, in at least two polarization frames, as well as a frame-invariant polarization parameter, $\tilde{\lambda} = (\lambda_\vartheta + 3\lambda_\varphi)/(1 - \lambda_\varphi)$ [10–12]. This approach was followed in the Y polarization analysis of CDF [13], in recent theoretical calculations [14], in the detailed study of the $Y(1S)$, $Y(2S)$, and $Y(3S)$ polarizations performed by CMS [15], and in the recent measurements of the J/ψ polarization at forward rapidity reported by ALICE [16] and LHCb [17]. This Letter presents the analogous measurement of the polarizations of the J/ψ and $\psi(2S)$ mesons (abbreviated as $\psi(nS)$, with $n = 1, 2$) promptly produced in pp collisions at a centre-of-mass energy of 7 TeV, at the LHC. The analysis is based on a dimuon sample collected in 2011, corresponding to an integrated luminosity of 4.9 fb^{-1} . The J/ψ ($\psi(2S)$) $\vec{\lambda}$ parameters are determined in several p_T bins in the range 14–70 GeV (14–50 GeV) and in two (three) absolute rapidity bins. Such a double-differential analysis is important to avoid obtaining diluted results from integrating over events characterized by significantly different kinematics [8].

The results correspond to the polarizations of the prompt $\psi(nS)$ states. The nonprompt component, mostly from decays of B mesons, is explicitly removed by using a proper-lifetime measurement. A significant fraction of the J/ψ prompt cross section is caused by feed-down decays from the $\psi(2S)$ (more than 8%, increasing with p_T) and from the χ_c (more than 25%) [18]. There are no feed-down decays from heavier charmonium states to the $\psi(2S)$ state, making it particularly interesting and easier to compare the measured polarization of this state with theoretical calculations. The polarization extraction method uses the dimuon invariant-mass distribution to separate the $\psi(nS)$ signal contributions from the continuum muon pairs from other processes (mostly pairs of muons resulting from decays of uncorrelated heavy-flavour mesons).

The two-dimensional shape of the decay angular distribution (in $\cos\theta$ and φ) is used to extract the three frame-dependent anisotropy parameters in three polarization frames, characterized by different choices of the quantization axis in the production plane: the centre-of-mass helicity (HX) frame, where the z axis coincides with the direction of the $\psi(nS)$ momentum in the laboratory; the Collins–Soper (CS) frame [19], whose z axis is the bisector of the two beam directions in the $\psi(nS)$ rest frame; and the perpendicular helicity (PX) frame [20], with the z axis orthogonal to that in the CS frame. The y axis is taken, in all cases, to be in the direction of the vector product of the two beam directions in the charmonium rest frame, $\vec{P}_1 \times \vec{P}_2$ and $\vec{P}_2 \times \vec{P}_1$ for positive and negative dimuon rapidities, respectively. More details regarding these frames are provided in Ref. [8]. The parameter $\tilde{\lambda}$, introduced in Ref. [11] to provide an alternative and frame-independent characterization of the quarkonium polarization properties, is measured simultaneously with the other parameters. This multidimensional approach reduces and keeps under control the smearing effects of the (unavoidable) partial averaging of the results over the range of the production and decay kinematics. This is important to minimize the possible interpretation ambiguities in the comparison with theoretical predictions and other experimental measurements [8].

2 CMS detector and data processing

The CMS apparatus [21] was designed around a central element: a superconducting solenoid of 6 m internal diameter, providing a 3.8 T field. Within the solenoid volume are a silicon pixel and strip tracker, a lead tungstate crystal electromagnetic calorimeter, and a brass/scintillator hadron calorimeter. Muons are measured in gas-ionization detectors embedded in the steel return yoke outside the solenoid and made using three technologies: drift tubes, cathode strip chambers, and resistive plate chambers. Extensive forward calorimetry complements the coverage provided by the barrel and endcap detectors. The main subdetectors used in this analysis are the silicon tracker and the muon system, which enable the measurement of muon momenta over the pseudorapidity range $|\eta| < 2.4$.

The events were collected using a two-level trigger system. The first level consists of custom hardware processors and uses information from the muon system to select events with two muons. The “high-level trigger” significantly reduces the number of events written to permanent storage by requiring an opposite-sign muon pair that fulfills certain kinematic conditions: invariant mass $2.8 < M < 3.35$ GeV, $p_T > 9.9$ GeV, and $|y| < 1.25$ for the J/ψ trigger; $3.35 < M < 4.05$ GeV and $p_T > 6.9$ GeV for the $\psi(2S)$ trigger. There is no rapidity requirement on the $\psi(2S)$ trigger, given its lower cross section, permitting an extra bin at forward rapidity with respect to the J/ψ case. No p_T requirement is imposed on the single muons at trigger level, only on the dimuon. Both triggers require a dimuon vertex-fit χ^2 probability greater than 0.5%. Events where the two muons bend towards each other in the magnetic field are rejected to lower the trigger rate while retaining the events where the dimuon detection efficiencies are most reliable.

The dimuons are reconstructed by combining two opposite-sign muons. The muon tracks are required to have hits in at least 11 tracker layers, at least two of which should be in the silicon pixel detector, and to be matched with at least one segment in the muon system. They must have a good track-fit quality (χ^2 per degree of freedom smaller than 1.8) and point to the interaction region. The selected muons must also be close, in pseudorapidity and azimuthal angle, to the muon objects responsible for triggering the event. In order to ensure accurately measured muon detection efficiencies, the analysis is restricted to muons produced within the range $|\eta| < 1.6$ and having transverse momentum above 4.5, 3.5, and 3.0 GeV for $|\eta| < 1.2$,

$1.2 < |\eta| < 1.4$, and $1.4 < |\eta| < 1.6$, respectively. The continuum background due to pairs of uncorrelated muons is reduced by requiring a dimuon vertex-fit χ^2 probability larger than 1%. After applying all event selection criteria and background removal, the total numbers of prompt plus nonprompt J/ψ events are 2.3 M and 2.4 M in the rapidity bins $|y| < 0.6$ and $0.6 < |y| < 1.2$, respectively. The corresponding $\psi(2S)$ yields are 126 k, 136 k, and 55 k for $|y| < 0.6$, $0.6 < |y| < 1.2$, and $1.2 < |y| < 1.5$, respectively. In each of these $|y|$ ranges, the analysis is performed in several p_T bins, with boundaries at 14, 16, 18, 20, 22, 25, 30, 35, 40, 50, and 70 GeV for the J/ψ , and 14, 18, 22, 30, and 50 GeV for the $\psi(2S)$.

The single-muon detection efficiencies are measured by a tag-and-probe technique [22], using event samples collected with dedicated triggers enriched in dimuons from J/ψ decays, where a muon is combined with a track and the pair is required to have an invariant mass within the range 2.8–3.4 GeV. The measurement procedure has been validated in the fiducial region of the analysis with detailed Monte Carlo (MC) simulation studies. The single-muon efficiencies are precisely measured and parametrized as a function of p_T , in eight $|\eta|$ bins, to avoid biases in the angular distributions that could mimic polarization effects. Their uncertainties, reflecting the statistical precision of the tag-and-probe samples and possible imperfections of the parametrization, contribute to the systematic uncertainty in the polarization measurement. At high dimuon p_T , when the two decay muons might be emitted relatively close to each other, the dimuon trigger has a lower efficiency than the simple product of the two single-muon efficiencies. Detailed MC simulations, validated with data collected with single-muon and dimuon triggers, are used to correct these trigger-induced muon-pair correlations.

3 Extraction of the polarization parameters

For each $\psi(nS)$ ($p_T, |y|$) bin, the dimuon invariant-mass distribution is fitted, using an unbinned maximum-likelihood fit, with an exponential function representing the underlying continuum background and two Crystal Ball (CB) functions [23] representing each peak. The two CB functions have independent widths, σ_{CB_1} and σ_{CB_2} , to accommodate the changing dimuon invariant-mass resolution within the rapidity cells, but share the same mean μ_{CB} and tail factors α_{CB} and n_{CB} (the latter fixed to 2.5).

Figure 1 shows two representative dimuon invariant-mass distributions in specific kinematic bins of the analysis. The dimuon invariant-mass resolution σ at the $\psi(nS)$ masses is evaluated from the fitted signal shapes, as $\sqrt{f_{CB_1}\sigma_{CB_1}^2 + (1 - f_{CB_1})\sigma_{CB_2}^2}$, where f_{CB_1} is the relative weight of the CB_1 function. The p_T -integrated values are $\sigma_{J/\psi} = 21$ and 32 MeV for $|y| < 0.6$ and $0.6 < |y| < 1.2$, respectively, and $\sigma_{\psi(nS)} = 25, 37$, and 48 MeV for $|y| < 0.6$, $0.6 < |y| < 1.2$, and $1.2 < |y| < 1.5$, respectively. For each ($p_T, |y|$) bin, the measured mass resolution is used to define a $\pm 3\sigma$ signal window around the resonance mass [24], m , as well as two mass sidebands, at lower and higher masses: from 2.85 GeV to $m_{J/\psi} - 4\sigma_{J/\psi}$ and from $m_{J/\psi} + 3.5\sigma_{J/\psi}$ to 3.3 GeV for the J/ψ ; from 3.4 GeV to $m_{\psi(2S)} - 4\sigma_{\psi(2S)}$ and from $m_{\psi(2S)} + 3.5\sigma_{\psi(2S)}$ to 4 GeV for the $\psi(2S)$. The larger gap in the low-mass sideband definition compared to the high-mass sideband minimizes the signal contamination induced by the low-mass tail of the signal peaks. The result of the invariant-mass fit provides the fraction of continuum-background events.

To minimize the fraction of charmonia from B decays in the sample used for the polarization measurement, a “prompt-signal region” is defined using the dimuon pseudo-proper lifetime [25], $\ell = L_{xy} \cdot m_{\psi(nS)} / p_T$, where L_{xy} is the transverse decay length in the laboratory frame. The measurement of L_{xy} is performed after removing the two muon tracks from the calculation of the primary vertex position; in the case of events with multiple collision vertices (pileup),

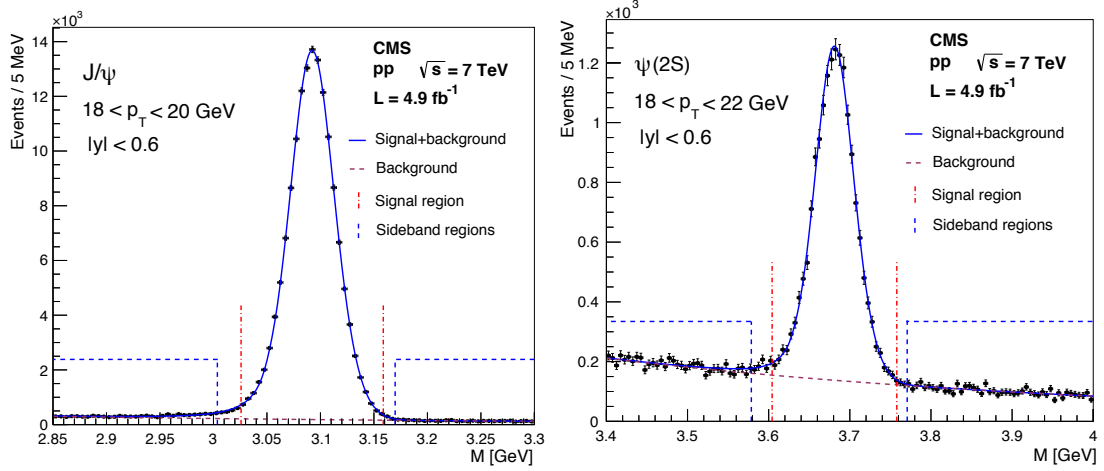


Figure 1: Dimuon invariant-mass distribution in the J/ψ (left) and $\psi(2S)$ (right) regions for an intermediate p_T bin and $|y| < 0.6$. The vertical lines delimit the signal region (dot-dashed) and the mass sidebands (dashed). The results of the fits are shown by the solid (signal+background) and dashed (background only) curves.

we select the one closest to the direction of the dimuon momentum, extrapolated towards the beam line.

The modelling of the resolution of the pseudo-proper lifetime exploits the per-event uncertainty information provided by the vertex reconstruction algorithm. The prompt-signal component is modelled by the resolution function, the nonprompt component by an exponential decay function convolved with the resolution function, and the continuum-background component by the sum of three exponential functions, also convolved with the resolution function. This composite model describes the data well with a relatively small number of free parameters. The systematic uncertainties induced by the lifetime fit in the polarization measurement are negligible. Figure 2 shows representative pseudo-proper-lifetime distributions for dimuons in the $\psi(nS)$ signal regions, together with the results of unbinned maximum-likelihood fits, performed simultaneously in the signal region and mass sidebands.

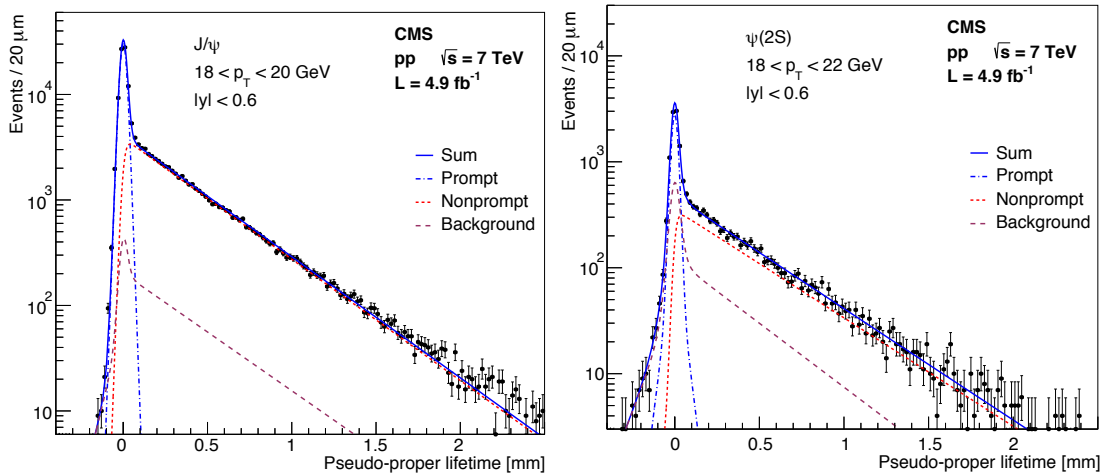


Figure 2: Pseudo-proper-lifetime distribution in the J/ψ (left) and $\psi(2S)$ (right) mass regions for intermediate p_T bins and $|y| < 0.6$. The results of the fits are shown by the solid curve, representing the sum of three contributions: prompt (dash-dotted), nonprompt (dotted), and background (dashed).

The prompt-signal regions, dominated by prompt charmonium events, are defined as $\pm 3\sigma_\ell$ signal windows around $\ell = 0$, where the lifetime resolution, σ_ℓ , is measured to be (for the phase space probed in this analysis) in the range 12–25 μm , improving with increasing dimuon p_T . The fractions of charmonia from B decays (f_{NP}) and continuum-background events (f_{B}) included in these regions are shown in Fig. 3 versus the dimuon p_T , for $|y| < 0.6$.

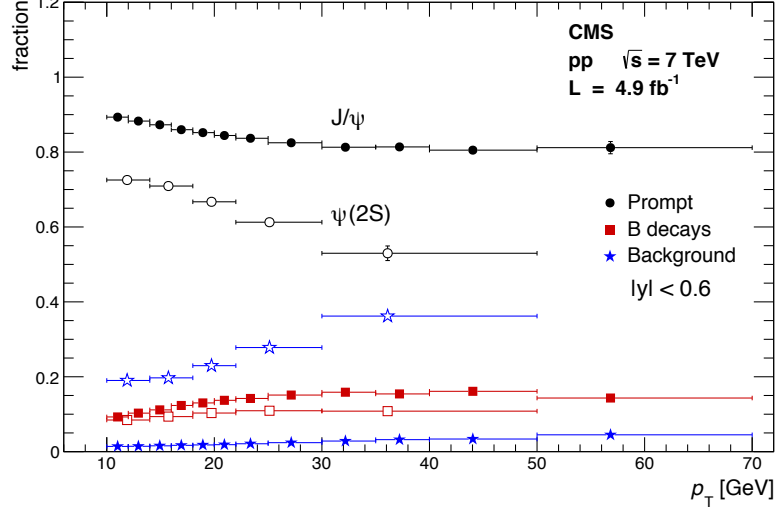


Figure 3: Fractions of prompt charmonium (circles), charmonium from B decays (squares), and continuum-background (stars) events in the prompt-signal mass-lifetime J/ψ (closed symbols) and $\psi(2S)$ (open symbols) regions versus the dimuon p_T for $|y| < 0.6$. A sideband subtraction technique removes the B and continuum backgrounds from the polarization analysis.

For each $\psi(nS)$ state, the angular distribution of the continuum background is modelled as the weighted sum of the distributions measured in the two mass sidebands (restricted to the prompt-lifetime region), with weights derived under the assumption that the background distribution changes linearly with the dimuon mass. This assumption is validated by comparing the (small) differences of the effective background polarizations measured in the four dimuon invariant-mass sidebands. The angular distribution of the $\psi(nS)$ from B decays is modelled using the events in the $\psi(nS)$ mass peak belonging to the “nonprompt-lifetime region”, $\ell > 3\sigma_\ell$, after subtracting the corresponding continuum-background contribution, interpolated from the nonprompt mass-sideband regions. As a cross-check of the analysis, the polarization of the nonprompt component was also measured, in two lifetime regions ($\ell > 3\sigma_\ell$ and $\ell > 5\sigma_\ell$), with consistent results.

The total background is the sum of the continuum-background and charmonia from B decays present in the prompt-signal region. To remove the background component, a fraction $f_{\text{B,tot}} = f_{\text{B}} + f_{\text{NP}}$ of the events is randomly selected by a procedure based on the likelihood-ratio $L_{\text{B}}/L_{\text{S+B}}$, where L_{B} ($L_{\text{S+B}}$) is the likelihood for an event under the background-only (signal-plus-background) hypothesis. This selection operates in such a way that the chosen events are distributed according to the $(p_T, |y|, M, \cos\theta, \varphi)$ distribution of the background model. The randomly selected events are removed from the sample.

The remaining (signal-like) events are used to calculate the posterior probability density (PPD) of the prompt- $\psi(nS)$ polarization parameters ($\vec{\lambda}$) for each kinematic bin,

$$\mathcal{P}(\vec{\lambda}) = \prod_i \mathcal{E}(\vec{p}_1^{(i)}, \vec{p}_2^{(i)}), \quad (2)$$

where \mathcal{E} is the probability density as a function of the two muon momenta $\vec{p}_{1,2}$ in event i . Uniform priors are used in the full $\vec{\lambda}$ parameter space. Many previous polarization measurements were dependent on assumptions made about the production kinematics because of the use of simulated acceptance and efficiency dilepton $(\cos \vartheta, \varphi)$ maps, averaged over all events in the considered kinematic cell. This analysis, instead, uses the efficiencies measured as a function of muon momentum, attributing to each event a probability dependent on the full event kinematics (not only on $\cos \vartheta$ and φ) and on the values of the polarization parameters. The event probability is calculated as

$$\mathcal{E}(\vec{p}_1, \vec{p}_2) = \frac{1}{\mathcal{N}(\vec{\lambda})} W(\cos \vartheta, \varphi | \vec{\lambda}) \epsilon(\vec{p}_1, \vec{p}_2), \quad (3)$$

where W is defined in Eq. (1) and $\epsilon(\vec{p}_1, \vec{p}_2)$ is the dimuon detection efficiency. The $\mathcal{N}(\vec{\lambda})$ normalization factor is obtained from integrating $W \epsilon$ over $\cos \vartheta$ and φ ,

$$\begin{aligned} \mathcal{N} = \frac{1}{(3 + \lambda_\vartheta)} & \left[\left(\iint \epsilon(\vec{p}_1, \vec{p}_2) \, d \cos \vartheta \, d\varphi \right) + \right. \\ & + \lambda_\vartheta \left(\iint \cos^2 \vartheta \, \epsilon(\vec{p}_1, \vec{p}_2) \, d \cos \vartheta \, d\varphi \right) + \\ & + \lambda_\varphi \left(\iint \sin^2 \vartheta \cos 2\varphi \, \epsilon(\vec{p}_1, \vec{p}_2) \, d \cos \vartheta \, d\varphi \right) + \\ & \left. + \lambda_{\vartheta\varphi} \left(\iint \sin 2\vartheta \cos \varphi \, \epsilon(\vec{p}_1, \vec{p}_2) \, d \cos \vartheta \, d\varphi \right) \right]. \quad (4) \end{aligned}$$

To perform this integration, $\epsilon(\vec{p}_1, \vec{p}_2)$ is expressed in terms of $\cos \vartheta$ and φ using the background-removed $(p_T, |y|, M)$ distributions. The background-removal procedure is repeated 50 times to minimize the statistical fluctuations associated with its random nature, and the PPD is obtained as the average of the 50 individual densities. The value 50 is very conservative; 20 iterations would have been sufficient to provide stable results.

Figure 4 illustrates the measured $\cos \vartheta$ and φ distributions in the HX frame for the case of J/ψ signal events in the kinematic bin $|y| < 0.6$ and $18 < p_T < 20$ GeV, after background removal. The data points are compared to curves reflecting the “best fit” (solid lines) as well as two extreme scenarios (dashed and dotted lines), corresponding to the λ_ϑ , λ_φ , and $\lambda_{\vartheta\varphi}$ values reported in the legends of the plots.

Most of the systematic uncertainties we have considered were studied and quantified (for each charmonium and each kinematic bin) with pseudo-experiments based on simulated events. Each test evaluates a specific systematic uncertainty and uses 50 statistically independent event samples, individually generated and reconstructed. The difference between the median of the 50 obtained polarization parameters and the injected values provides the systematic uncertainty corresponding to the effect under study. In particular, several signal and background polarization scenarios have been used to evaluate the reliability of the analysis framework, including extreme signal polarizations in the highest- p_T bins of the analysis, where the dimuon trigger inefficiency has the strongest effect. Possible residual biases in the muon or dimuon efficiencies, resulting from the tag-and-probe measurement precision or from the efficiency parametrization, could affect the extraction of the polarization parameters. This effect is evaluated by applying uncertainty-based changes to the used efficiencies. The systematic uncertainty resulting from the unknown background angular distribution under the signal peak is evaluated using the measured data, by changing the relative weights of the low- and high-mass sidebands in the background model between 0.25 and 0.75, very different from the measured

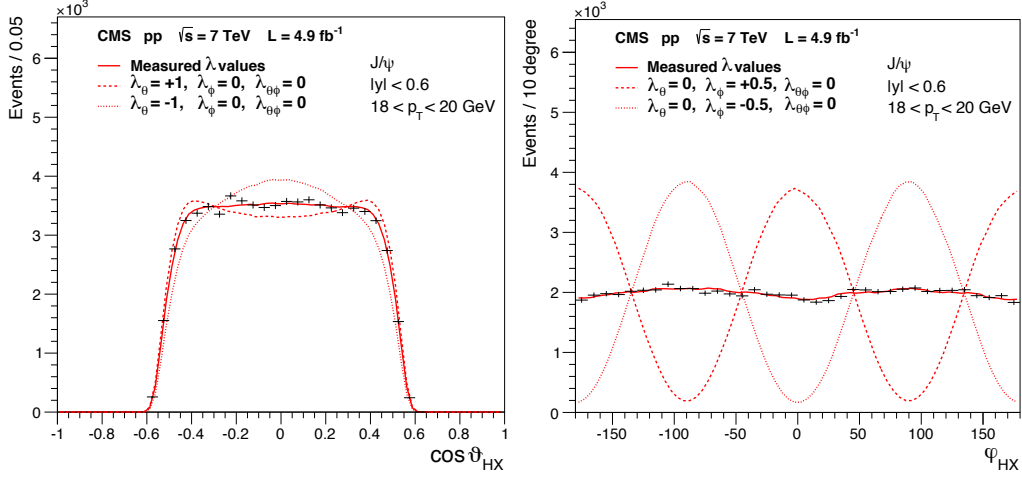


Figure 4: Frequency distributions of $\cos \theta$ (left) and φ (right) angular variables, in the HX frame for the J/ψ in an intermediate p_T bin and $|y| < 0.6$. The curves represent the expected distributions for two extreme polarization scenarios (dashed and dotted lines defined in the legends) and for the measured $\bar{\lambda}$ (solid lines).

values of ≈ 0.5 . The resulting uncertainty is negligible, as expected given the small magnitude of the background and the proximity of the mass sidebands to the charmonia peaks. The systematic uncertainty associated with the definition of the prompt-signal region is evaluated as the difference between the MC simulation results obtained with a $\pm 3\sigma_\ell$ window and with no pseudo-proper-lifetime requirement.

The $\psi(2S)$ polarization uncertainties are dominated by statistics limitations in all $(p_T, |y|)$ bins. In the J/ψ case, at high p_T the uncertainties are dominated by the statistical accuracy, while for $p_T \lesssim 30$ GeV they are determined by systematic effects. The largest among these include the single-muon ($\approx 0.1, 0.02$, and 0.03) and dimuon ($\approx 0.05, 0.03$, and 0.02) efficiencies, and the prompt-region definition ($\approx 0.03, 0.02$, and 0.01); the values given correspond to the systematic uncertainties for λ_θ , λ_φ , and $\lambda_{\theta\varphi}$, respectively, in the HX frame, averaged over the rapidity bins.

The final PPD of the polarization parameters is the average of the PPDs corresponding to all hypotheses considered in the determination of the systematic uncertainties. The central value of each polarization parameter, for each kinematic bin, is evaluated as the mode of the associated one-dimensional marginal posterior, which is calculated by numerical integration. The corresponding uncertainties, at a given confidence level (CL), are given by the $[\lambda_1, \lambda_2]$ intervals, defined such that each of the regions $[-\infty, \lambda_1]$ and $[\lambda_2, \infty]$ integrates to half of $(1 - \text{CL})$ of the marginal PPD. Two-dimensional marginal posteriors provide information about correlations between the measurements of the three λ parameters. As an example, Fig. 5 shows the two-dimensional marginals for λ_φ vs. λ_θ (left) and $\lambda_{\theta\varphi}$ vs. λ_φ (right) measured from J/ψ at $|y| < 0.6$ and $18 < p_T < 20$ GeV, displaying the 68.3% and 99.7% CL contours for the CS and PX frames. The figure also indicates the physically allowed regions for the decay of a $J = 1$ particle; this region does not affect the calculation of the PPD anywhere in the analysis. For visibility reasons, the HX curves are not shown; in the phase space of this analysis (mid-rapidity and relatively high p_T), the HX and PX frames are almost identical.

4 Results

The frame-dependent λ parameters measured in the HX frame are presented, for both charmonia, in Fig. 6, as a function of p_T and $|y|$. The average values of p_T and $|y|$ are given in Table 1 of

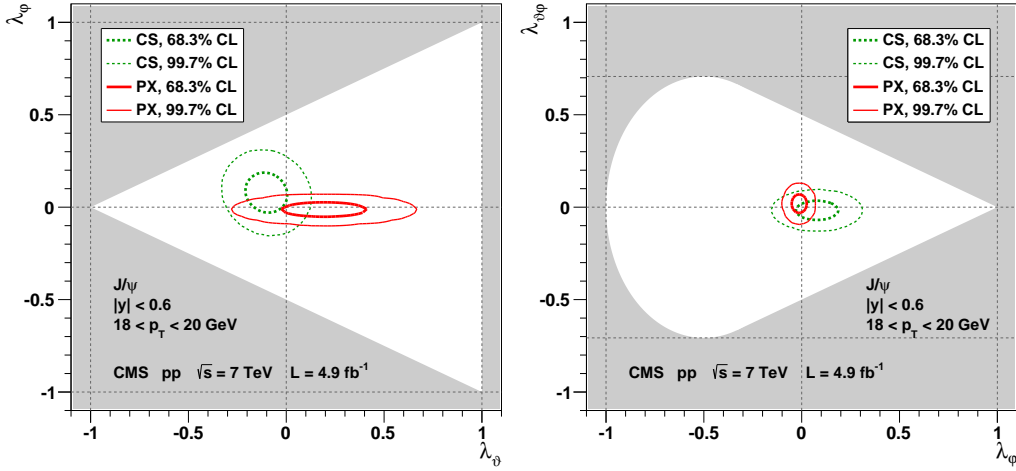


Figure 5: Two-dimensional marginals of the PPD in the λ_ϕ vs. λ_θ (left) and $\lambda_{\theta\phi}$ vs. λ_ϕ (right) planes, for J/ψ with $|y| < 0.6$ and $18 < p_T < 20$ GeV. The 68.3% and 99.7% CL total uncertainties are shown for the CS and PX frames. The shaded areas represent physically forbidden regions of parameter space [12].

Appendix A for each kinematic bin. The solid curves in the top two panels of Fig. 6 represent next-to-leading order (NLO) NRQCD calculations [26] of the λ_θ parameter for prompt J/ψ and $\psi(2S)$ mesons as a function of p_T for $|y| < 2.4$. The dashed lines give an estimate of the uncertainties in the theoretical predictions. The measured values of λ_θ are in clear disagreement with these NLO NRQCD calculations. Figure 7 displays the frame-invariant parameter, $\tilde{\lambda}$, measured in the CS, HX, and PX frames, for the rapidity range $|y| < 0.6$. The three sets of $\tilde{\lambda}$ measurements are in good agreement, as required in the absence of unaddressed systematic effects; the same consistency is also observed in the other rapidity bins. All the results for λ_θ , λ_ϕ , $\lambda_{\theta\phi}$, and $\tilde{\lambda}$, for the two $\psi(nS)$ states and in the three frames considered in this analysis, including the total 68.3%, 95.5%, and 99.7% CL uncertainties and the 68.3% CL statistical uncertainties, are tabulated in Appendix A.

None of the three polarization frames shows large polarizations, excluding the possibility that a significant polarization could remain undetected because of smearing effects induced by inappropriate frame choices [8]. While a small prompt J/ψ polarization can be interpreted as reflecting a mixture of directly produced mesons with those produced in the decays of heavier (P-wave) charmonium states, this explanation cannot apply to the $\psi(2S)$ state, unaffected by feed-down decays from heavier charmonia.

5 Summary

In summary, the polarizations of prompt J/ψ and $\psi(2S)$ mesons produced in pp collisions at $\sqrt{s} = 7$ TeV have been determined as a function of the $\psi(nS)$ p_T in two or three rapidity ranges, extending well beyond the domains probed by previous experiments, and in three different polarization frames, using both frame-dependent and frame-independent parameters. All the measured λ parameters are close to zero, excluding large polarizations in the explored kinematic regions. These results are in clear disagreement with existing NLO NRQCD calculations [26–28] and provide a good basis for significant improvements in the understanding of quarkonium production in high-energy hadron collisions.

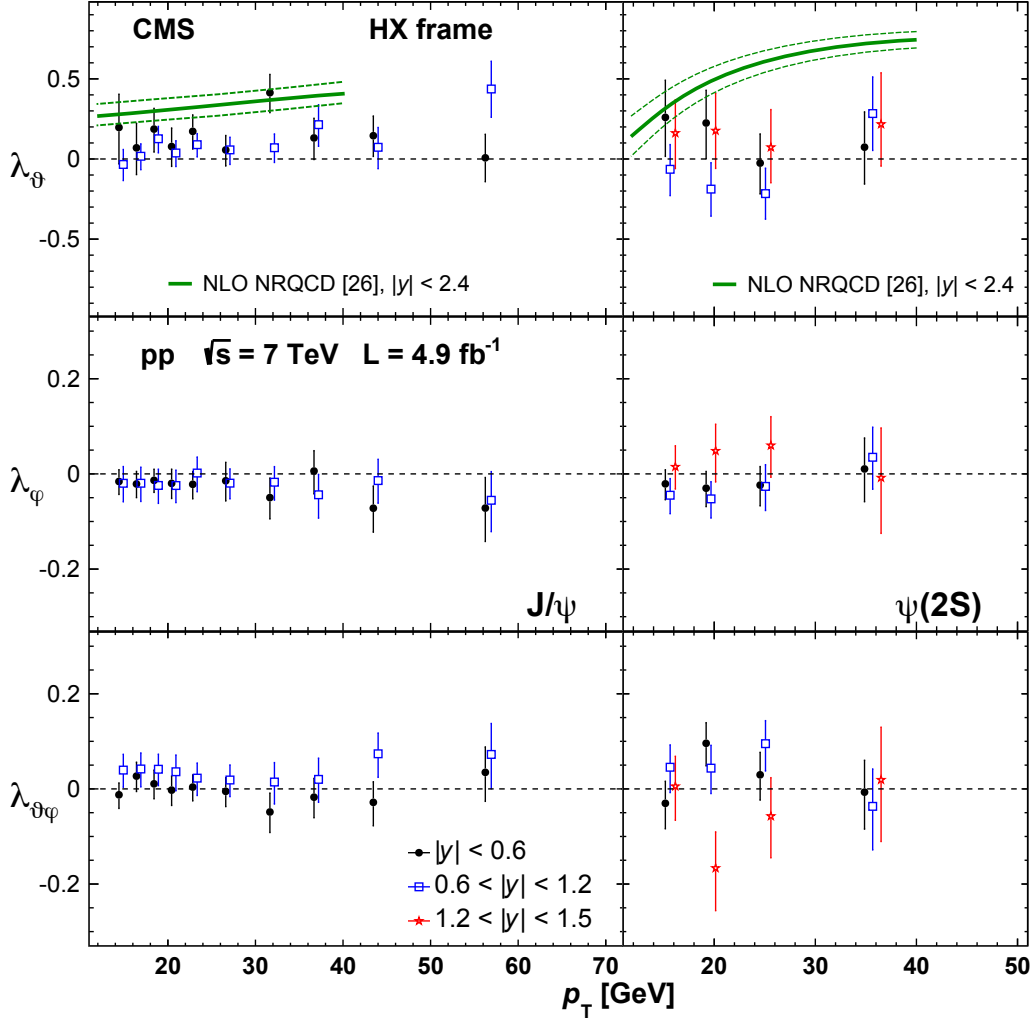


Figure 6: Polarization parameters λ_θ , λ_ϕ , and $\lambda_{\theta\phi}$ measured in the HX frame for prompt J/ψ (left) and $\psi(2S)$ (right) mesons, as a function of p_T and for several $|y|$ bins. The error bars represent total uncertainties (at 68.3% CL). The curves in the top two panels represent calculations of λ_θ from NLO NRQCD [26], the dashed lines illustrating their uncertainties.

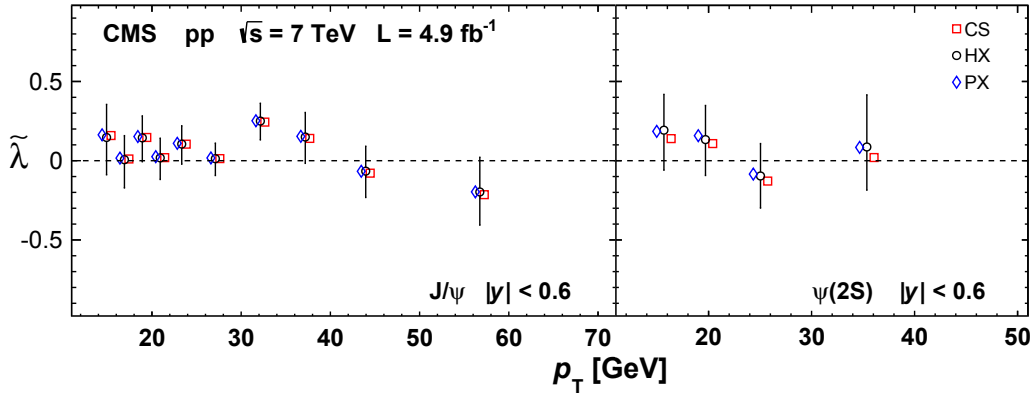


Figure 7: Values of the frame-independent parameter $\tilde{\lambda}$ for the J/ψ (left) and $\psi(2S)$ (right) measured in the CS, HX, and PX frames, as a function of p_T and for $|y| < 0.6$. The error bars represent total uncertainties (at 68.3% CL).

Acknowledgements

We congratulate our colleagues in the CERN accelerator departments for the excellent performance of the LHC and thank the technical and administrative staffs at CERN and at other CMS institutes for their contributions to the success of the CMS effort. In addition, we gratefully acknowledge the computing centres and personnel of the Worldwide LHC Computing Grid for delivering so effectively the computing infrastructure essential to our analyses. Finally, we acknowledge the enduring support for the construction and operation of the LHC and the CMS detector provided by the following funding agencies: BMWF and FWF (Austria); FNRS and FWO (Belgium); CNPq, CAPES, FAPERJ, and FAPESP (Brazil); MEYS (Bulgaria); CERN; CAS, MoST, and NSFC (China); COLCIENCIAS (Colombia); MSES (Croatia); RPF (Cyprus); MoER, SF0690030s09 and ERDF (Estonia); Academy of Finland, MEC, and HIP (Finland); CEA and CNRS/IN2P3 (France); BMBF, DFG, and HGF (Germany); GSRT (Greece); OTKA and NKTH (Hungary); DAE and DST (India); IPM (Iran); SFI (Ireland); INFN (Italy); NRF and WCU (Republic of Korea); LAS (Lithuania); CINVESTAV, CONACYT, SEP, and UASLP-FAI (Mexico); MSI (New Zealand); PAEC (Pakistan); MSHE and NSC (Poland); FCT (Portugal); JINR (Armenia, Belarus, Georgia, Ukraine, Uzbekistan); MON, RosAtom, RAS and RFBR (Russia); MSTD (Serbia); SEIDI and CPAN (Spain); Swiss Funding Agencies (Switzerland); NSC (Taipei); ThEP-Center, IPST and NSTDA (Thailand); TUBITAK and TAEK (Turkey); NASU (Ukraine); STFC (United Kingdom); DOE and NSF (USA). Individuals have received support from the Marie-Curie programme and the European Research Council and EPLANET (European Union); the Leventis Foundation; the A.P. Sloan Foundation; the Alexander von Humboldt Foundation; the Belgian Federal Science Policy Office; the Fonds pour la Formation à la Recherche dans l'Industrie et dans l'Agriculture (FRIA-Belgium); the Agentschap voor Innovatie door Wetenschap en Technologie (IWT-Belgium); the Ministry of Education, Youth and Sports (MEYS) of Czech Republic; the Council of Science and Industrial Research, India; the Compagnia di San Paolo (Torino); the HOMING PLUS programme of Foundation for Polish Science, cofinanced by EU, Regional Development Fund; and the Thalís and Aristeia programmes cofinanced by EU-ESF and the Greek NSRF.

References

- [1] N. Brambilla et al., “Heavy quarkonium: progress, puzzles, and opportunities”, *Eur. Phys. J. C* **71** (2011) 1534, doi:10.1140/epjc/s10052-010-1534-9, arXiv:1010.5827.
- [2] G. T. Bodwin, E. Braaten, and G. P. Lepage, “Rigorous QCD analysis of inclusive annihilation and production of heavy quarkonium”, *Phys. Rev. D* **51** (1995) 1125, doi:10.1103/PhysRevD.55.5853, arXiv:hep-ph/9407339.
- [3] J.-P. Lansberg, “On the mechanisms of heavy-quarkonium hadroproduction”, *Eur. Phys. J. C* **61** (2009) 693, doi:10.1140/epjc/s10052-008-0826-9, arXiv:0811.4005.
- [4] M. Beneke and M. Kramer, “Direct J/ψ and ψ' polarization and cross-sections at the Tevatron”, *Phys. Rev. D* **55** (1997) 5269, doi:10.1103/PhysRevD.55.5269, arXiv:hep-ph/9611218.
- [5] A. K. Leibovich, “ ψ' polarization due to color-octet quarkonia production”, *Phys. Rev. D* **56** (1997) 4412, doi:10.1103/PhysRevD.56.4412, arXiv:hep-ph/9610381.

- [6] E. Braaten, B. A. Kniehl, and J. Lee, "Polarization of prompt J/ψ at the Fermilab Tevatron", *Phys. Rev. D* **62** (2000) 094005, doi:10.1103/PhysRevD.62.094005, arXiv:hep-ph/9911436.
- [7] CDF Collaboration, "Polarization of J/ψ and $\psi(2S)$ mesons produced in $p\bar{p}$ collisions at $\sqrt{s} = 1.96$ TeV", *Phys. Rev. Lett.* **99** (2007) 132001, doi:10.1103/PhysRevLett.99.132001, arXiv:0704.0638.
- [8] P. Faccioli, C. Lourenço, J. Seixas, and H. K. Wöhri, "Towards the experimental clarification of quarkonium polarization", *Eur. Phys. J. C* **69** (2010) 657, doi:10.1140/epjc/s10052-010-1420-5, arXiv:1006.2738.
- [9] P. Faccioli, C. Lourenço, J. Seixas, and H. K. Wöhri, "J/ ψ Polarization from Fixed-Target to Collider Energies", *Phys. Rev. Lett.* **102** (2009) 151802, doi:10.1103/PhysRevLett.102.151802, arXiv:0902.4462.
- [10] P. Faccioli, C. Lourenço, and J. Seixas, "Rotation-invariant relations in vector meson decays into fermion pairs", *Phys. Rev. Lett.* **105** (2010) 061601, doi:10.1103/PhysRevLett.105.061601, arXiv:1005.2601.
- [11] P. Faccioli, C. Lourenço, and J. Seixas, "New approach to quarkonium polarization studies", *Phys. Rev. D* **81** (2010) 111502(R), doi:10.1103/PhysRevD.81.111502, arXiv:1005.2855.
- [12] P. Faccioli, C. Lourenço, J. Seixas, and H. K. Wöhri, "Model-independent constraints on the shape parameters of dilepton angular distributions", *Phys. Rev. D* **83** (2011) 056008, doi:10.1103/PhysRevD.83.056008, arXiv:1102.3946.
- [13] CDF Collaboration, "Measurements of Angular Distributions of Muons from Y Meson Decays in $p\bar{p}$ Collisions at $\sqrt{s} = 1.96$ TeV", *Phys. Rev. Lett.* **108** (2012) 151802, doi:10.1103/PhysRevLett.108.151802, arXiv:1112.1591.
- [14] S. P. Baranov, A. V. Lipatov, and N. P. Zotov, "Prompt J/ψ production at LHC: new evidence for the k_T -factorization", *Phys. Rev. D* **85** (2012) 014034, doi:10.1103/PhysRevD.85.014034, arXiv:1108.2856.
- [15] CMS Collaboration, "Measurement of the Y(1S), Y(2S), and Y(3S) polarizations in pp collisions at $\sqrt{s} = 7$ TeV", *Phys. Rev. Lett.* **110** (2013) 081802, doi:10.1103/PhysRevLett.110.081802, arXiv:1209.2922.
- [16] ALICE Collaboration, "J/ ψ polarization in pp collisions at $\sqrt{s} = 7$ TeV", *Phys. Rev. Lett.* **108** (2012) 082001, doi:10.1103/PhysRevLett.108.082001, arXiv:1111.1630.
- [17] LHCb Collaboration, "Measurement of J/ ψ polarization in pp collisions at $\sqrt{s} = 7$ TeV", (2013). arXiv:1307.6379.
- [18] P. Faccioli, C. Lourenço, J. Seixas, and H. K. Wöhri, "Study of ψ' and χ_c decays as feed-down sources of J/ ψ hadro-production", *JHEP* **10** (2008) 004, doi:10.1088/1126-6708/2008/10/004, arXiv:0809.2153.
- [19] J. C. Collins and D. E. Soper, "Angular Distribution of Dileptons in High-Energy Hadron Collisions", *Phys. Rev. D* **16** (1977) 2219, doi:10.1103/PhysRevD.16.2219.

- [20] E. Braaten, D. Kang, J. Lee, and C. Yu, "Optimal spin quantization axes for the polarization of dileptons with large transverse momentum", *Phys. Rev. D* **79** (2009) 014025, doi:10.1103/PhysRevD.79.014025, arXiv:0810.4506.
- [21] CMS Collaboration, "The CMS experiment at the CERN LHC", *JINST* **03** (2008) S08004, doi:10.1088/1748-0221/3/08/S08004.
- [22] CMS Collaboration, "Measurements of Inclusive W and Z Cross Sections in pp Collisions at $\sqrt{s} = 7$ TeV", *JHEP* **01** (2011) 080, doi:10.1007/JHEP01(2011)080, arXiv:1012.2466.
- [23] M. J. Oreglia, "A study of the reactions $\psi' \rightarrow \gamma\gamma\psi$ ". PhD thesis, Stanford University, 1980. SLAC Report SLAC-R-236.
- [24] Particle Data Group, J. Beringer et al., "Review of Particle Physics", *Phys. Rev. D* **86** (2012) 010001, doi:10.1103/PhysRevD.86.010001.
- [25] CMS Collaboration, "Prompt and non-prompt J/ ψ production in pp collisions at $\sqrt{s} = 7$ TeV", *Eur. Phys. J. C* **71** (2011) 1575, doi:10.1140/epjc/s10052-011-1575-8, arXiv:1011.4193.
- [26] B. Gong, L.-P. Wan, J.-X. Wang, and H.-F. Zhang, "Polarization for Prompt J/ ψ , $\psi(2S)$ production at the Tevatron and LHC", *Phys. Rev. Lett.* **110** (2013) 042002, doi:10.1103/PhysRevLett.110.042002, arXiv:1205.6682.
- [27] M. Butenschoen and B. A. Kniehl, "J/ ψ polarization at Tevatron and LHC: Nonrelativistic-QCD factorization at the crossroads", *Phys. Rev. Lett.* **108** (2012) 172002, doi:10.1103/PhysRevLett.108.172002, arXiv:1201.1872.
- [28] K.-T. Chao et al., "J/ ψ Polarization at Hadron Colliders in Nonrelativistic QCD", *Phys. Rev. Lett.* **108** (2012) 242004, doi:10.1103/PhysRevLett.108.242004, arXiv:1201.2675.

A Supplemental material

Table 1 gives the average values of p_T and $|y|$ for each kinematical bin. Tables 2–25 list the results of the angular anisotropy parameters λ_θ , λ_φ , and $\lambda_{\theta\varphi}$, and the frame-invariant parameter $\tilde{\lambda}$, for the two $\psi(nS)$ states in the Collins-Soper (CS), helicity (HX), and perpendicular helicity (PX) frames, along with their total uncertainties (68.3%, 95.5%, and 99.7% CL) and statistical uncertainties only (68.3% CL) in different bins of $\psi(nS)$ transverse momentum p_T and absolute rapidity $|y|$.

Table 1: Average p_T (in GeV) and $|y|$, for each $\psi(nS)$ kinematical bin.

p_T (GeV)	$0.0 < y < 0.6$		$0.6 < y < 1.2$		$1.2 < y < 1.5$	
	$\langle p_T \rangle$	$\langle y \rangle$	$\langle p_T \rangle$	$\langle y \rangle$	$\langle p_T \rangle$	$\langle y \rangle$
J/ψ						
10–12	11.0	0.30	11.0	0.92	–	–
12–14	12.9	0.30	12.9	0.91	–	–
14–16	14.9	0.30	14.9	0.90	–	–
16–18	16.9	0.30	16.9	0.90	–	–
18–20	18.9	0.30	18.9	0.89	–	–
20–22	20.9	0.30	20.9	0.89	–	–
22–25	23.3	0.30	23.3	0.89	–	–
25–30	27.1	0.30	27.1	0.89	–	–
30–35	32.2	0.30	32.2	0.89	–	–
35–40	37.2	0.30	37.2	0.88	–	–
40–50	44.0	0.30	44.0	0.89	–	–
50–70	56.8	0.30	56.9	0.88	–	–
$\psi(2S)$						
10–14	11.9	0.30	11.8	0.92	11.8	1.33
14–18	15.7	0.30	15.6	0.90	15.7	1.33
18–22	19.7	0.30	19.7	0.89	19.6	1.33
22–30	25.0	0.31	25.1	0.88	25.1	1.34
30–50	35.4	0.31	35.7	0.89	36.0	1.34

Table 2: λ_θ in the CS frame for the J/ψ .

$ y $	p_T (GeV)	λ_θ	Total uncertainty			Stat. unc.
			68.3% CL	95.5% CL	99.7% CL	68.3% CL
0.0–0.6	14–16	−0.116	+0.102 −0.116	+0.210 −0.224	+0.319 −0.333	+0.024 −0.025
	16–18	−0.062	+0.082 −0.088	+0.167 −0.173	+0.251 −0.258	+0.024 −0.024
	18–20	−0.102	+0.066 −0.073	+0.135 −0.139	+0.201 −0.208	+0.025 −0.026
	20–22	−0.066	+0.058 −0.063	+0.121 −0.126	+0.181 −0.187	+0.028 −0.028
	22–25	−0.107	+0.055 −0.061	+0.114 −0.117	+0.169 −0.175	+0.027 −0.027
	25–30	−0.049	+0.080 −0.088	+0.163 −0.172	+0.252 −0.260	+0.029 −0.029
	30–35	−0.227	+0.087 −0.094	+0.175 −0.182	+0.263 −0.270	+0.033 −0.033
	35–40	−0.048	+0.104 −0.114	+0.214 −0.218	+0.323 −0.321	+0.057 −0.057
	40–50	−0.154	+0.098 −0.105	+0.197 −0.204	+0.296 −0.298	+0.058 −0.057
	50–70	−0.084	+0.128 −0.137	+0.271 −0.266	+0.407 −0.387	+0.095 −0.087
0.6–1.2	14–16	+0.003	+0.052 −0.058	+0.106 −0.111	+0.162 −0.168	+0.023 −0.025
	16–18	−0.017	+0.046 −0.051	+0.097 −0.100	+0.145 −0.151	+0.024 −0.025
	18–20	−0.074	+0.046 −0.051	+0.095 −0.099	+0.143 −0.145	+0.023 −0.023
	20–22	−0.039	+0.046 −0.051	+0.096 −0.099	+0.146 −0.146	+0.030 −0.030
	22–25	−0.029	+0.045 −0.049	+0.092 −0.096	+0.142 −0.141	+0.028 −0.029
	25–30	−0.049	+0.051 −0.054	+0.104 −0.108	+0.158 −0.162	+0.028 −0.029
	30–35	−0.051	+0.053 −0.059	+0.112 −0.114	+0.168 −0.167	+0.040 −0.042
	35–40	−0.141	+0.095 −0.103	+0.189 −0.198	+0.288 −0.292	+0.051 −0.051
	40–50	−0.033	+0.096 −0.104	+0.204 −0.206	+0.306 −0.303	+0.070 −0.065
	50–70	−0.217	+0.110 −0.118	+0.227 −0.222	+0.344 −0.327	+0.088 −0.081

Table 3: λ_ϕ in the CS frame for the J/ψ .

$ y $	p_T (GeV)	λ_ϕ	Total uncertainty			Stat. unc.
			68.3% CL	95.5% CL	99.7% CL	68.3% CL
0.0–0.6	14–16	+0.087	+0.099 –0.112	+0.204 –0.217	+0.309 –0.322	+0.022 –0.027
	16–18	+0.024	+0.075 –0.084	+0.156 –0.165	+0.238 –0.247	+0.022 –0.027
	18–20	+0.079	+0.064 –0.073	+0.135 –0.143	+0.202 –0.210	+0.022 –0.027
	20–22	+0.028	+0.059 –0.066	+0.118 –0.128	+0.181 –0.187	+0.025 –0.031
	22–25	+0.068	+0.054 –0.062	+0.113 –0.119	+0.170 –0.179	+0.024 –0.027
	25–30	+0.020	+0.049 –0.056	+0.103 –0.110	+0.157 –0.163	+0.023 –0.027
	30–35	+0.145	+0.052 –0.058	+0.107 –0.113	+0.159 –0.168	+0.027 –0.032
	35–40	+0.060	+0.063 –0.072	+0.133 –0.142	+0.198 –0.211	+0.040 –0.046
	40–50	+0.026	+0.063 –0.073	+0.133 –0.143	+0.199 –0.213	+0.041 –0.047
	50–70	–0.045	+0.079 –0.091	+0.164 –0.177	+0.245 –0.262	+0.060 –0.067
0.6–1.2	14–16	–0.031	+0.057 –0.061	+0.113 –0.120	+0.172 –0.179	+0.023 –0.026
	16–18	–0.010	+0.048 –0.053	+0.099 –0.104	+0.150 –0.155	+0.021 –0.025
	18–20	+0.040	+0.049 –0.054	+0.102 –0.107	+0.152 –0.158	+0.020 –0.024
	20–22	–0.001	+0.046 –0.050	+0.094 –0.101	+0.140 –0.149	+0.024 –0.030
	22–25	+0.037	+0.045 –0.049	+0.090 –0.098	+0.136 –0.144	+0.022 –0.027
	25–30	+0.015	+0.042 –0.048	+0.087 –0.094	+0.131 –0.137	+0.022 –0.026
	30–35	+0.021	+0.048 –0.053	+0.099 –0.106	+0.149 –0.157	+0.031 –0.036
	35–40	+0.068	+0.064 –0.072	+0.131 –0.144	+0.199 –0.212	+0.038 –0.044
	40–50	+0.018	+0.065 –0.076	+0.138 –0.149	+0.207 –0.221	+0.044 –0.054
	50–70	+0.141	+0.072 –0.084	+0.150 –0.162	+0.224 –0.244	+0.054 –0.062

Table 4: $\lambda_{\vartheta\varphi}$ in the CS frame for the J/ψ .

$ y $	p_T (GeV)	$\lambda_{\vartheta\varphi}$	Total uncertainty			Stat. unc.
			68.3% CL	95.5% CL	99.7% CL	68.3% CL
0.0–0.6	14–16	+0.001	+0.031 –0.034	+0.063 –0.066	+0.094 –0.099	+0.008 –0.009
	16–18	–0.030	+0.031 –0.034	+0.065 –0.069	+0.097 –0.101	+0.009 –0.010
	18–20	–0.017	+0.031 –0.035	+0.064 –0.068	+0.096 –0.100	+0.011 –0.011
	20–22	–0.001	+0.030 –0.034	+0.062 –0.066	+0.093 –0.098	+0.012 –0.013
	22–25	–0.009	+0.026 –0.030	+0.054 –0.057	+0.081 –0.085	+0.012 –0.014
	25–30	+0.003	+0.026 –0.029	+0.054 –0.056	+0.082 –0.085	+0.014 –0.015
	30–35	+0.029	+0.035 –0.039	+0.072 –0.076	+0.110 –0.114	+0.019 –0.021
	35–40	+0.014	+0.036 –0.042	+0.077 –0.080	+0.115 –0.118	+0.028 –0.030
	40–50	+0.022	+0.041 –0.046	+0.085 –0.089	+0.131 –0.133	+0.029 –0.032
	50–70	–0.035	+0.054 –0.059	+0.108 –0.113	+0.164 –0.169	+0.046 –0.050
0.6–1.2	14–16	–0.035	+0.034 –0.038	+0.071 –0.073	+0.105 –0.109	+0.009 –0.009
	16–18	–0.044	+0.031 –0.035	+0.065 –0.068	+0.097 –0.100	+0.009 –0.009
	18–20	–0.054	+0.028 –0.031	+0.057 –0.061	+0.087 –0.090	+0.010 –0.011
	20–22	–0.040	+0.032 –0.036	+0.066 –0.070	+0.101 –0.105	+0.012 –0.014
	22–25	–0.028	+0.032 –0.035	+0.065 –0.068	+0.097 –0.101	+0.013 –0.014
	25–30	–0.023	+0.031 –0.034	+0.063 –0.066	+0.095 –0.100	+0.014 –0.015
	30–35	–0.020	+0.038 –0.044	+0.080 –0.085	+0.122 –0.125	+0.020 –0.023
	35–40	–0.031	+0.040 –0.045	+0.081 –0.086	+0.123 –0.127	+0.027 –0.030
	40–50	–0.074	+0.042 –0.047	+0.088 –0.093	+0.132 –0.139	+0.032 –0.036
	50–70	–0.073	+0.055 –0.061	+0.110 –0.116	+0.165 –0.171	+0.046 –0.051

Table 5: $\tilde{\lambda}$ in the CS frame for the J/ψ .

$ y $	p_T (GeV)	$\tilde{\lambda}$	Total uncertainty			Stat. unc.
			68.3% CL	95.5% CL	99.7% CL	68.3% CL
0.0–0.6	14–16	+0.159	+0.208 –0.234	+0.428 –0.454	+0.649 –0.675	+0.057 –0.063
	16–18	+0.011	+0.145 –0.168	+0.306 –0.321	+0.458 –0.481	+0.051 –0.058
	18–20	+0.147	+0.134 –0.153	+0.285 –0.297	+0.429 –0.441	+0.059 –0.062
	20–22	+0.019	+0.135 –0.144	+0.277 –0.286	+0.413 –0.429	+0.063 –0.065
	22–25	+0.104	+0.116 –0.124	+0.236 –0.244	+0.356 –0.364	+0.066 –0.066
	25–30	+0.013	+0.097 –0.105	+0.199 –0.206	+0.300 –0.307	+0.060 –0.063
	30–35	+0.244	+0.119 –0.123	+0.243 –0.241	+0.367 –0.353	+0.097 –0.092
	35–40	+0.141	+0.156 –0.167	+0.327 –0.320	+0.497 –0.465	+0.130 –0.124
	40–50	–0.079	+0.163 –0.171	+0.330 –0.329	+0.506 –0.478	+0.126 –0.117
	50–70	–0.214	+0.219 –0.206	+0.456 –0.407	+0.692 –0.596	+0.189 –0.152
0.6–1.2	14–16	–0.088	+0.104 –0.118	+0.218 –0.226	+0.332 –0.339	+0.047 –0.049
	16–18	–0.047	+0.098 –0.107	+0.203 –0.207	+0.303 –0.312	+0.046 –0.047
	18–20	+0.047	+0.092 –0.105	+0.196 –0.204	+0.294 –0.302	+0.050 –0.051
	20–22	–0.041	+0.088 –0.097	+0.183 –0.192	+0.273 –0.282	+0.056 –0.060
	22–25	+0.087	+0.096 –0.103	+0.193 –0.205	+0.296 –0.302	+0.058 –0.062
	25–30	–0.005	+0.086 –0.093	+0.178 –0.185	+0.270 –0.272	+0.059 –0.060
	30–35	+0.011	+0.115 –0.118	+0.234 –0.231	+0.354 –0.338	+0.091 –0.085
	35–40	+0.068	+0.155 –0.164	+0.322 –0.315	+0.490 –0.458	+0.128 –0.120
	40–50	+0.017	+0.165 –0.167	+0.344 –0.328	+0.524 –0.480	+0.146 –0.133
	50–70	+0.223	+0.264 –0.224	+0.528 –0.448	+0.831 –0.646	+0.243 –0.195

Table 6: λ_ϑ in the HX frame for the J/ ψ .

$ y $	p_T (GeV)	λ_ϑ	Total uncertainty			Stat. unc.
			68.3% CL	95.5% CL	99.7% CL	68.3% CL
0.0–0.6	14–16	+0.197	+0.208 –0.228	+0.419 –0.439	+0.630 –0.651	+0.055 –0.061
	16–18	+0.070	+0.153 –0.167	+0.313 –0.336	+0.473 –0.496	+0.051 –0.055
	18–20	+0.187	+0.129 –0.143	+0.259 –0.273	+0.395 –0.409	+0.053 –0.059
	20–22	+0.078	+0.116 –0.124	+0.233 –0.247	+0.356 –0.364	+0.055 –0.059
	22–25	+0.172	+0.103 –0.110	+0.212 –0.220	+0.316 –0.329	+0.058 –0.061
	25–30	+0.056	+0.090 –0.100	+0.188 –0.198	+0.286 –0.295	+0.050 –0.054
	30–35	+0.414	+0.114 –0.125	+0.230 –0.241	+0.347 –0.357	+0.078 –0.083
	35–40	+0.131	+0.123 –0.135	+0.258 –0.257	+0.387 –0.386	+0.095 –0.093
	40–50	+0.145	+0.123 –0.129	+0.252 –0.252	+0.389 –0.375	+0.098 –0.095
	50–70	+0.007	+0.147 –0.149	+0.303 –0.281	+0.466 –0.414	+0.123 –0.120
0.6–1.2	14–16	–0.034	+0.093 –0.100	+0.190 –0.197	+0.287 –0.294	+0.048 –0.049
	16–18	+0.017	+0.078 –0.084	+0.158 –0.165	+0.239 –0.245	+0.046 –0.047
	18–20	+0.126	+0.077 –0.088	+0.158 –0.168	+0.243 –0.249	+0.047 –0.051
	20–22	+0.037	+0.077 –0.085	+0.159 –0.167	+0.242 –0.250	+0.052 –0.058
	22–25	+0.089	+0.069 –0.077	+0.146 –0.153	+0.218 –0.226	+0.050 –0.054
	25–30	+0.057	+0.079 –0.091	+0.166 –0.174	+0.249 –0.257	+0.049 –0.051
	30–35	+0.070	+0.086 –0.092	+0.175 –0.177	+0.264 –0.261	+0.069 –0.070
	35–40	+0.214	+0.125 –0.135	+0.258 –0.262	+0.391 –0.388	+0.095 –0.093
	40–50	+0.073	+0.124 –0.133	+0.256 –0.259	+0.394 –0.378	+0.099 –0.100
	50–70	+0.437	+0.173 –0.177	+0.362 –0.337	+0.561 –0.498	+0.165 –0.151

Table 7: λ_φ in the HX frame for the J/ ψ .

$ y $	p_T (GeV)	λ_φ	Total uncertainty			Stat. unc.
			68.3% CL	95.5% CL	99.7% CL	68.3% CL
0.0–0.6	14–16	−0.016	+0.025 −0.027	+0.051 −0.053	+0.077 −0.079	+0.004 −0.005
	16–18	−0.021	+0.026 −0.029	+0.054 −0.056	+0.082 −0.084	+0.005 −0.006
	18–20	−0.014	+0.023 −0.025	+0.047 −0.050	+0.072 −0.074	+0.006 −0.007
	20–22	−0.020	+0.030 −0.032	+0.059 −0.063	+0.090 −0.093	+0.008 −0.009
	22–25	−0.022	+0.027 −0.031	+0.056 −0.058	+0.084 −0.088	+0.009 −0.010
	25–30	−0.015	+0.039 −0.042	+0.077 −0.081	+0.118 −0.121	+0.010 −0.011
	30–35	−0.050	+0.041 −0.045	+0.084 −0.088	+0.127 −0.131	+0.017 −0.019
	35–40	+0.006	+0.043 −0.048	+0.089 −0.095	+0.134 −0.139	+0.025 −0.028
	40–50	−0.072	+0.047 −0.050	+0.095 −0.101	+0.144 −0.150	+0.030 −0.033
	50–70	−0.072	+0.064 −0.070	+0.132 −0.141	+0.199 −0.205	+0.047 −0.053
0.6–1.2	14–16	−0.020	+0.035 −0.039	+0.070 −0.074	+0.107 −0.111	+0.005 −0.005
	16–18	−0.020	+0.034 −0.038	+0.070 −0.074	+0.108 −0.110	+0.005 −0.006
	18–20	−0.024	+0.034 −0.038	+0.070 −0.074	+0.104 −0.108	+0.007 −0.007
	20–22	−0.024	+0.032 −0.036	+0.066 −0.070	+0.099 −0.102	+0.009 −0.010
	22–25	+0.002	+0.034 −0.039	+0.071 −0.075	+0.107 −0.110	+0.010 −0.011
	25–30	−0.019	+0.030 −0.033	+0.062 −0.065	+0.093 −0.098	+0.011 −0.012
	30–35	−0.017	+0.033 −0.038	+0.070 −0.073	+0.105 −0.108	+0.018 −0.019
	35–40	−0.044	+0.043 −0.049	+0.090 −0.094	+0.135 −0.139	+0.026 −0.029
	40–50	−0.014	+0.045 −0.048	+0.091 −0.094	+0.137 −0.140	+0.032 −0.034
	50–70	−0.055	+0.060 −0.066	+0.122 −0.127	+0.187 −0.192	+0.054 −0.057

Table 8: $\lambda_{\vartheta\varphi}$ in the HX frame for the J/ψ .

$ y $	p_T (GeV)	$\lambda_{\vartheta\varphi}$	Total uncertainty			Stat. unc.
			68.3% CL	95.5% CL	99.7% CL	68.3% CL
0.0–0.6	14–16	−0.012	+0.025 −0.029	+0.053 −0.055	+0.079 −0.082	+0.010 −0.011
	16–18	+0.027	+0.029 −0.032	+0.060 −0.063	+0.091 −0.094	+0.010 −0.011
	18–20	+0.011	+0.029 −0.032	+0.057 −0.062	+0.088 −0.092	+0.011 −0.013
	20–22	−0.003	+0.030 −0.032	+0.059 −0.063	+0.090 −0.094	+0.013 −0.014
	22–25	+0.004	+0.026 −0.029	+0.054 −0.057	+0.080 −0.084	+0.014 −0.015
	25–30	−0.005	+0.029 −0.032	+0.059 −0.062	+0.090 −0.093	+0.014 −0.016
	30–35	−0.049	+0.040 −0.043	+0.081 −0.087	+0.125 −0.128	+0.023 −0.025
	35–40	−0.017	+0.040 −0.043	+0.082 −0.086	+0.122 −0.126	+0.030 −0.033
	40–50	−0.028	+0.043 −0.049	+0.090 −0.096	+0.136 −0.142	+0.032 −0.037
	50–70	+0.035	+0.053 −0.061	+0.112 −0.117	+0.168 −0.175	+0.046 −0.050
0.6–1.2	14–16	+0.040	+0.033 −0.036	+0.068 −0.071	+0.103 −0.105	+0.009 −0.009
	16–18	+0.042	+0.034 −0.038	+0.069 −0.073	+0.105 −0.109	+0.009 −0.010
	18–20	+0.041	+0.032 −0.035	+0.065 −0.068	+0.098 −0.101	+0.011 −0.012
	20–22	+0.036	+0.035 −0.040	+0.074 −0.079	+0.111 −0.115	+0.013 −0.014
	22–25	+0.023	+0.032 −0.036	+0.066 −0.071	+0.100 −0.105	+0.013 −0.015
	25–30	+0.019	+0.032 −0.035	+0.065 −0.068	+0.097 −0.102	+0.014 −0.016
	30–35	+0.014	+0.041 −0.046	+0.084 −0.090	+0.128 −0.131	+0.021 −0.023
	35–40	+0.020	+0.045 −0.048	+0.089 −0.095	+0.135 −0.139	+0.031 −0.034
	40–50	+0.074	+0.044 −0.050	+0.090 −0.096	+0.137 −0.143	+0.034 −0.036
	50–70	+0.072	+0.065 −0.072	+0.130 −0.137	+0.195 −0.202	+0.054 −0.062

Table 9: $\tilde{\lambda}$ in the HX frame for the J/ψ .

$ y $	p_T (GeV)	$\tilde{\lambda}$	Total uncertainty			Stat. unc.
			68.3% CL	95.5% CL	99.7% CL	68.3% CL
0.0–0.6	14–16	+0.147	+0.209 –0.236	+0.437 –0.464	+0.665 –0.692	+0.056 –0.064
	16–18	+0.006	+0.152 –0.178	+0.326 –0.343	+0.491 –0.509	+0.051 –0.057
	18–20	+0.144	+0.139 –0.151	+0.280 –0.299	+0.428 –0.440	+0.055 –0.060
	20–22	+0.018	+0.124 –0.136	+0.254 –0.266	+0.377 –0.397	+0.060 –0.064
	22–25	+0.105	+0.116 –0.127	+0.240 –0.245	+0.358 –0.369	+0.063 –0.066
	25–30	+0.013	+0.098 –0.106	+0.203 –0.211	+0.302 –0.310	+0.058 –0.060
	30–35	+0.250	+0.112 –0.119	+0.234 –0.235	+0.356 –0.344	+0.092 –0.093
	35–40	+0.150	+0.155 –0.166	+0.324 –0.318	+0.493 –0.470	+0.127 –0.121
	40–50	–0.066	+0.157 –0.166	+0.328 –0.328	+0.508 –0.481	+0.123 –0.117
	50–70	–0.197	+0.219 –0.209	+0.451 –0.406	+0.694 –0.603	+0.184 –0.155
0.6–1.2	14–16	–0.091	+0.105 –0.114	+0.214 –0.224	+0.330 –0.333	+0.050 –0.047
	16–18	–0.041	+0.090 –0.100	+0.187 –0.193	+0.284 –0.290	+0.046 –0.048
	18–20	+0.052	+0.092 –0.101	+0.184 –0.193	+0.280 –0.289	+0.049 –0.053
	20–22	–0.035	+0.086 –0.093	+0.172 –0.183	+0.261 –0.268	+0.057 –0.059
	22–25	+0.095	+0.091 –0.100	+0.182 –0.191	+0.278 –0.287	+0.057 –0.061
	25–30	–0.002	+0.081 –0.090	+0.170 –0.179	+0.258 –0.262	+0.057 –0.058
	30–35	+0.017	+0.111 –0.122	+0.231 –0.230	+0.357 –0.344	+0.088 –0.087
	35–40	+0.079	+0.151 –0.161	+0.319 –0.313	+0.479 –0.457	+0.121 –0.117
	40–50	+0.030	+0.166 –0.173	+0.340 –0.328	+0.524 –0.484	+0.142 –0.128
	50–70	+0.248	+0.252 –0.227	+0.532 –0.453	+0.825 –0.653	+0.239 –0.201

Table 10: λ_θ in the PX frame for the J/ψ .

$ y $	p_T (GeV)	λ_θ	Total uncertainty			Stat. unc.
			68.3% CL	95.5% CL	99.7% CL	68.3% CL
0.0–0.6	14–16	+0.215	+0.208 –0.227	+0.425 –0.444	+0.642 –0.661	+0.058 –0.062
	16–18	+0.076	+0.155 –0.173	+0.319 –0.337	+0.475 –0.501	+0.049 –0.055
	18–20	+0.193	+0.134 –0.148	+0.275 –0.289	+0.423 –0.438	+0.056 –0.059
	20–22	+0.086	+0.114 –0.128	+0.233 –0.246	+0.351 –0.365	+0.057 –0.062
	22–25	+0.177	+0.108 –0.119	+0.221 –0.232	+0.335 –0.346	+0.057 –0.061
	25–30	+0.062	+0.093 –0.101	+0.193 –0.201	+0.293 –0.301	+0.051 –0.052
	30–35	+0.420	+0.115 –0.130	+0.241 –0.250	+0.361 –0.369	+0.079 –0.083
	35–40	+0.137	+0.123 –0.131	+0.254 –0.261	+0.391 –0.385	+0.093 –0.094
	40–50	+0.145	+0.122 –0.130	+0.256 –0.256	+0.389 –0.375	+0.098 –0.096
	50–70	+0.001	+0.144 –0.147	+0.301 –0.289	+0.465 –0.423	+0.125 –0.115
0.6–1.2	14–16	–0.044	+0.101 –0.107	+0.203 –0.214	+0.310 –0.316	+0.048 –0.050
	16–18	–0.002	+0.084 –0.090	+0.169 –0.179	+0.258 –0.264	+0.044 –0.048
	18–20	+0.108	+0.080 –0.091	+0.171 –0.177	+0.257 –0.263	+0.048 –0.050
	20–22	+0.025	+0.083 –0.089	+0.169 –0.174	+0.254 –0.260	+0.050 –0.057
	22–25	+0.077	+0.073 –0.079	+0.149 –0.155	+0.225 –0.231	+0.049 –0.054
	25–30	+0.053	+0.075 –0.083	+0.154 –0.162	+0.237 –0.241	+0.048 –0.052
	30–35	+0.068	+0.089 –0.096	+0.179 –0.181	+0.274 –0.267	+0.068 –0.070
	35–40	+0.210	+0.127 –0.139	+0.264 –0.268	+0.400 –0.390	+0.096 –0.096
	40–50	+0.062	+0.123 –0.135	+0.259 –0.257	+0.394 –0.380	+0.099 –0.101
	50–70	+0.427	+0.174 –0.177	+0.364 –0.339	+0.563 –0.491	+0.164 –0.151

Table 11: λ_φ in the PX frame for the J/ψ .

$ y $	p_T (GeV)	λ_φ	Total uncertainty			Stat. unc.
			68.3% CL	95.5% CL	99.7% CL	68.3% CL
0.0–0.6	14–16	−0.016	+0.022 −0.025	+0.047 −0.048	+0.070 −0.073	+0.004 −0.005
	16–18	−0.020	+0.025 −0.028	+0.052 −0.055	+0.078 −0.082	+0.006 −0.006
	18–20	−0.013	+0.023 −0.026	+0.048 −0.049	+0.072 −0.074	+0.007 −0.007
	20–22	−0.020	+0.027 −0.031	+0.056 −0.059	+0.084 −0.087	+0.008 −0.009
	22–25	−0.022	+0.026 −0.029	+0.053 −0.055	+0.079 −0.083	+0.009 −0.010
	25–30	−0.015	+0.037 −0.042	+0.077 −0.082	+0.118 −0.120	+0.010 −0.011
	30–35	−0.051	+0.041 −0.045	+0.085 −0.089	+0.129 −0.133	+0.017 −0.019
	35–40	+0.005	+0.044 −0.049	+0.089 −0.094	+0.135 −0.139	+0.025 −0.028
	40–50	−0.072	+0.046 −0.052	+0.095 −0.099	+0.142 −0.148	+0.029 −0.032
	50–70	−0.071	+0.063 −0.073	+0.132 −0.138	+0.200 −0.206	+0.048 −0.053
0.6–1.2	14–16	−0.014	+0.032 −0.035	+0.065 −0.069	+0.099 −0.102	+0.004 −0.004
	16–18	−0.014	+0.031 −0.036	+0.065 −0.068	+0.097 −0.100	+0.005 −0.006
	18–20	−0.018	+0.032 −0.036	+0.064 −0.068	+0.099 −0.101	+0.007 −0.007
	20–22	−0.020	+0.026 −0.030	+0.056 −0.060	+0.084 −0.088	+0.009 −0.009
	22–25	+0.004	+0.030 −0.034	+0.064 −0.068	+0.096 −0.100	+0.010 −0.011
	25–30	−0.018	+0.030 −0.033	+0.061 −0.064	+0.093 −0.095	+0.011 −0.012
	30–35	−0.016	+0.033 −0.036	+0.065 −0.069	+0.099 −0.103	+0.017 −0.019
	35–40	−0.042	+0.044 −0.048	+0.089 −0.095	+0.136 −0.139	+0.026 −0.029
	40–50	−0.010	+0.043 −0.047	+0.087 −0.093	+0.134 −0.137	+0.031 −0.034
	50–70	−0.052	+0.061 −0.068	+0.122 −0.129	+0.187 −0.190	+0.052 −0.057

Table 12: $\lambda_{\theta\varphi}$ in the PX frame for the J/ψ .

$ y $	p_T (GeV)	$\lambda_{\theta\varphi}$	Total uncertainty			Stat. unc.
			68.3% CL	95.5% CL	99.7% CL	68.3% CL
0.0–0.6	14–16	+0.000	+0.032 –0.035	+0.066 –0.068	+0.099 –0.102	+0.010 –0.010
	16–18	+0.031	+0.031 –0.034	+0.064 –0.067	+0.096 –0.099	+0.010 –0.011
	18–20	+0.019	+0.032 –0.035	+0.063 –0.067	+0.097 –0.100	+0.011 –0.012
	20–22	+0.001	+0.030 –0.033	+0.061 –0.066	+0.094 –0.097	+0.013 –0.014
	22–25	+0.010	+0.027 –0.030	+0.054 –0.057	+0.083 –0.084	+0.013 –0.014
	25–30	–0.003	+0.028 –0.030	+0.057 –0.059	+0.086 –0.088	+0.014 –0.016
	30–35	–0.036	+0.038 –0.043	+0.080 –0.083	+0.121 –0.125	+0.023 –0.025
	35–40	–0.015	+0.040 –0.045	+0.082 –0.086	+0.125 –0.128	+0.029 –0.033
	40–50	–0.024	+0.044 –0.050	+0.090 –0.096	+0.135 –0.140	+0.032 –0.037
	50–70	+0.036	+0.055 –0.062	+0.112 –0.119	+0.169 –0.176	+0.046 –0.051
0.6–1.2	14–16	+0.035	+0.032 –0.036	+0.068 –0.072	+0.102 –0.106	+0.009 –0.009
	16–18	+0.044	+0.031 –0.035	+0.063 –0.066	+0.096 –0.100	+0.009 –0.010
	18–20	+0.057	+0.028 –0.030	+0.057 –0.061	+0.085 –0.089	+0.011 –0.012
	20–22	+0.041	+0.033 –0.037	+0.068 –0.072	+0.104 –0.106	+0.013 –0.014
	22–25	+0.030	+0.032 –0.035	+0.065 –0.068	+0.099 –0.102	+0.013 –0.015
	25–30	+0.024	+0.032 –0.035	+0.065 –0.068	+0.098 –0.100	+0.014 –0.015
	30–35	+0.020	+0.039 –0.044	+0.082 –0.087	+0.125 –0.130	+0.021 –0.023
	35–40	+0.035	+0.044 –0.049	+0.091 –0.094	+0.135 –0.140	+0.031 –0.034
	40–50	+0.077	+0.045 –0.050	+0.092 –0.097	+0.139 –0.144	+0.034 –0.036
	50–70	+0.090	+0.065 –0.070	+0.130 –0.136	+0.196 –0.201	+0.056 –0.061

Table 13: $\tilde{\lambda}$ in the PX frame for the J/ψ .

$ y $	p_T (GeV)	$\tilde{\lambda}$	Total uncertainty			Stat. unc.
			68.3% CL	95.5% CL	99.7% CL	68.3% CL
0.0–0.6	14–16	+0.163	+0.212 –0.238	+0.425 –0.451	+0.650 –0.676	+0.059 –0.062
	16–18	+0.016	+0.148 –0.163	+0.312 –0.327	+0.467 –0.483	+0.051 –0.058
	18–20	+0.153	+0.136 –0.148	+0.278 –0.297	+0.420 –0.439	+0.056 –0.060
	20–22	+0.025	+0.131 –0.146	+0.266 –0.281	+0.400 –0.416	+0.061 –0.067
	22–25	+0.110	+0.120 –0.134	+0.247 –0.261	+0.374 –0.388	+0.062 –0.066
	25–30	+0.017	+0.094 –0.108	+0.196 –0.204	+0.297 –0.306	+0.060 –0.062
	30–35	+0.252	+0.116 –0.122	+0.233 –0.232	+0.355 –0.348	+0.094 –0.092
	35–40	+0.154	+0.170 –0.173	+0.342 –0.344	+0.523 –0.506	+0.126 –0.120
	40–50	–0.067	+0.168 –0.176	+0.353 –0.344	+0.530 –0.512	+0.127 –0.116
	50–70	–0.197	+0.217 –0.225	+0.456 –0.428	+0.707 –0.619	+0.182 –0.152
0.6–1.2	14–16	–0.084	+0.107 –0.115	+0.221 –0.229	+0.335 –0.337	+0.051 –0.048
	16–18	–0.043	+0.097 –0.106	+0.196 –0.205	+0.295 –0.304	+0.046 –0.049
	18–20	+0.051	+0.093 –0.104	+0.189 –0.200	+0.290 –0.295	+0.049 –0.052
	20–22	–0.036	+0.085 –0.098	+0.177 –0.184	+0.268 –0.276	+0.055 –0.059
	22–25	+0.091	+0.086 –0.097	+0.178 –0.188	+0.269 –0.275	+0.056 –0.061
	25–30	–0.001	+0.081 –0.089	+0.166 –0.170	+0.246 –0.250	+0.057 –0.058
	30–35	+0.018	+0.110 –0.118	+0.230 –0.232	+0.350 –0.340	+0.086 –0.086
	35–40	+0.080	+0.164 –0.171	+0.331 –0.329	+0.507 –0.487	+0.126 –0.118
	40–50	+0.031	+0.176 –0.185	+0.361 –0.351	+0.546 –0.508	+0.143 –0.129
	50–70	+0.249	+0.256 –0.238	+0.537 –0.463	+0.833 –0.660	+0.239 –0.207

Table 14: λ_θ in the CS frame for the $\psi(2S)$.

$ y $	p_T (GeV)	λ_θ	Total uncertainty			Stat. unc. 68.3% CL
			68.3% CL	95.5% CL	99.7% CL	
0.0–0.6	14–18	−0.124	+0.105 −0.108	+0.224 −0.215	+0.342 −0.315	+0.078 −0.063
	18–22	−0.118	+0.107 −0.104	+0.215 −0.196	+0.339 −0.288	+0.086 −0.076
	22–30	−0.009	+0.113 −0.105	+0.237 −0.199	+0.367 −0.294	+0.103 −0.087
	30–50	+0.014	+0.163 −0.133	+0.346 −0.256	+0.573 −0.378	+0.154 −0.116
0.6–1.2	14–18	−0.002	+0.092 −0.091	+0.194 −0.177	+0.295 −0.263	+0.075 −0.064
	18–22	+0.048	+0.118 −0.101	+0.242 −0.201	+0.390 −0.290	+0.103 −0.081
	22–30	+0.123	+0.126 −0.114	+0.256 −0.218	+0.406 −0.316	+0.114 −0.099
	30–50	−0.066	+0.146 −0.116	+0.312 −0.227	+0.542 −0.322	+0.138 −0.103
1.2–1.5	14–18	−0.021	+0.123 −0.125	+0.250 −0.245	+0.384 −0.359	+0.086 −0.077
	18–22	−0.055	+0.144 −0.150	+0.303 −0.285	+0.470 −0.419	+0.118 −0.098
	22–30	+0.061	+0.171 −0.139	+0.347 −0.282	+0.548 −0.408	+0.154 −0.115
	30–50	−0.058	+0.213 −0.187	+0.442 −0.370	+0.705 −0.531	+0.194 −0.148

Table 15: λ_φ in the CS frame for the $\psi(2S)$.

$ y $	p_T (GeV)	λ_φ	Total uncertainty			Stat. unc. 68.3% CL
			68.3% CL	95.5% CL	99.7% CL	
0.0–0.6	14–18	+0.084	+0.098 −0.124	+0.210 −0.241	+0.309 −0.363	+0.057 −0.087
	18–22	+0.075	+0.084 −0.109	+0.172 −0.220	+0.255 −0.336	+0.064 −0.094
	22–30	−0.038	+0.087 −0.111	+0.177 −0.217	+0.263 −0.334	+0.071 −0.099
	30–50	+0.018	+0.095 −0.137	+0.197 −0.274	+0.293 −0.431	+0.083 −0.127
0.6–1.2	14–18	−0.076	+0.088 −0.103	+0.179 −0.209	+0.264 −0.315	+0.058 −0.083
	18–22	−0.155	+0.096 −0.125	+0.197 −0.244	+0.287 −0.376	+0.075 −0.106
	22–30	−0.161	+0.090 −0.120	+0.189 −0.237	+0.275 −0.361	+0.080 −0.112
	30–50	+0.129	+0.084 −0.115	+0.170 −0.222	+0.256 −0.345	+0.075 −0.103
1.2–1.5	14–18	+0.059	+0.093 −0.118	+0.196 −0.233	+0.293 −0.360	+0.064 −0.094
	18–22	+0.109	+0.092 −0.134	+0.191 −0.257	+0.278 −0.396	+0.078 −0.120
	22–30	+0.050	+0.103 −0.143	+0.208 −0.290	+0.314 −0.466	+0.089 −0.132
	30–50	+0.064	+0.115 −0.154	+0.246 −0.299	+0.362 −0.452	+0.111 −0.139

Table 16: $\lambda_{\theta\varphi}$ in the CS frame for the $\psi(2S)$.

$ y $	p_T (GeV)	$\lambda_{\theta\varphi}$	Total uncertainty			Stat. unc. 68.3% CL
			68.3% CL	95.5% CL	99.7% CL	
0.0–0.6	14–18	+0.012	+0.042 –0.045	+0.088 –0.089	+0.131 –0.131	+0.029 –0.029
	18–22	–0.098	+0.040 –0.046	+0.082 –0.090	+0.124 –0.135	+0.033 –0.039
	22–30	–0.029	+0.049 –0.053	+0.097 –0.104	+0.148 –0.152	+0.042 –0.046
	30–50	+0.006	+0.069 –0.078	+0.144 –0.149	+0.219 –0.220	+0.067 –0.070
0.6–1.2	14–18	–0.038	+0.045 –0.048	+0.092 –0.098	+0.141 –0.144	+0.027 –0.029
	18–22	–0.025	+0.046 –0.052	+0.096 –0.099	+0.144 –0.149	+0.037 –0.040
	22–30	–0.081	+0.052 –0.057	+0.107 –0.108	+0.161 –0.163	+0.045 –0.048
	30–50	+0.018	+0.076 –0.078	+0.154 –0.152	+0.231 –0.225	+0.066 –0.066
1.2–1.5	14–18	–0.028	+0.058 –0.064	+0.120 –0.122	+0.181 –0.180	+0.045 –0.047
	18–22	+0.134	+0.074 –0.077	+0.153 –0.149	+0.232 –0.221	+0.067 –0.066
	22–30	+0.056	+0.078 –0.085	+0.161 –0.168	+0.240 –0.247	+0.066 –0.074
	30–50	–0.033	+0.107 –0.117	+0.235 –0.226	+0.395 –0.335	+0.095 –0.102

Table 17: $\tilde{\lambda}$ in the CS frame for the $\psi(2S)$.

$ y $	p_T (GeV)	$\tilde{\lambda}$	Total uncertainty			Stat. unc. 68.3% CL
			68.3% CL	95.5% CL	99.7% CL	
0.0–0.6	14–18	+0.139	+0.232 –0.257	+0.482 –0.495	+0.733 –0.732	+0.172 –0.178
	18–22	+0.108	+0.225 –0.230	+0.458 –0.453	+0.692 –0.664	+0.191 –0.191
	22–30	–0.129	+0.207 –0.193	+0.423 –0.387	+0.650 –0.560	+0.190 –0.171
	30–50	+0.020	+0.321 –0.250	+0.678 –0.500	+1.160 –0.714	+0.316 –0.238
0.6–1.2	14–18	–0.214	+0.176 –0.186	+0.367 –0.367	+0.557 –0.548	+0.126 –0.128
	18–22	–0.365	+0.179 –0.183	+0.361 –0.355	+0.551 –0.509	+0.149 –0.141
	22–30	–0.323	+0.188 –0.176	+0.384 –0.344	+0.580 –0.502	+0.170 –0.153
	30–50	+0.328	+0.365 –0.277	+0.734 –0.533	+1.135 –0.774	+0.354 –0.254
1.2–1.5	14–18	+0.157	+0.229 –0.225	+0.468 –0.441	+0.708 –0.644	+0.207 –0.201
	18–22	+0.254	+0.331 –0.287	+0.664 –0.557	+1.013 –0.794	+0.317 –0.270
	22–30	+0.179	+0.346 –0.281	+0.710 –0.562	+1.089 –0.810	+0.329 –0.269
	30–50	+0.094	+0.492 –0.363	+1.015 –0.720	+1.680 –1.005	+0.469 –0.302

Table 18: λ_θ in the HX frame for the $\psi(2S)$.

$ y $	p_T (GeV)	λ_θ	Total uncertainty			Stat. unc. 68.3% CL
			68.3% CL	95.5% CL	99.7% CL	
0.0–0.6	14–18	+0.260	+0.232 –0.243	+0.470 –0.481	+0.707 –0.719	+0.165 –0.173
	18–22	+0.225	+0.204 –0.223	+0.429 –0.425	+0.643 –0.616	+0.180 –0.183
	22–30	–0.026	+0.182 –0.193	+0.384 –0.366	+0.585 –0.538	+0.162 –0.155
	30–50	+0.074	+0.220 –0.230	+0.457 –0.444	+0.718 –0.657	+0.208 –0.209
0.6–1.2	14–18	–0.064	+0.154 –0.164	+0.322 –0.324	+0.481 –0.475	+0.127 –0.133
	18–22	–0.188	+0.165 –0.169	+0.332 –0.336	+0.508 –0.485	+0.142 –0.147
	22–30	–0.216	+0.159 –0.160	+0.322 –0.307	+0.486 –0.446	+0.147 –0.139
	30–50	+0.284	+0.229 –0.230	+0.482 –0.436	+0.736 –0.641	+0.220 –0.210
1.2–1.5	14–18	+0.162	+0.208 –0.222	+0.423 –0.425	+0.638 –0.629	+0.169 –0.171
	18–22	+0.177	+0.233 –0.236	+0.480 –0.458	+0.726 –0.656	+0.222 –0.216
	22–30	+0.073	+0.235 –0.222	+0.476 –0.438	+0.728 –0.643	+0.216 –0.211
	30–50	+0.217	+0.321 –0.262	+0.667 –0.498	+1.061 –0.719	+0.322 –0.240

Table 19: λ_ϕ in the HX frame for the $\psi(2S)$.

$ y $	p_T (GeV)	λ_ϕ	Total uncertainty			Stat. unc. 68.3% CL
			68.3% CL	95.5% CL	99.7% CL	
0.0–0.6	14–18	–0.021	+0.030 –0.033	+0.061 –0.065	+0.094 –0.098	+0.013 –0.015
	18–22	–0.030	+0.035 –0.039	+0.073 –0.077	+0.111 –0.115	+0.024 –0.025
	22–30	–0.024	+0.039 –0.044	+0.081 –0.086	+0.122 –0.126	+0.030 –0.033
	30–50	+0.010	+0.065 –0.069	+0.130 –0.131	+0.203 –0.193	+0.057 –0.060
0.6–1.2	14–18	–0.045	+0.035 –0.039	+0.074 –0.078	+0.111 –0.115	+0.014 –0.015
	18–22	–0.052	+0.036 –0.040	+0.074 –0.079	+0.115 –0.117	+0.022 –0.023
	22–30	–0.026	+0.046 –0.051	+0.091 –0.096	+0.139 –0.142	+0.032 –0.034
	30–50	+0.035	+0.063 –0.067	+0.132 –0.129	+0.207 –0.191	+0.057 –0.060
1.2–1.5	14–18	+0.015	+0.044 –0.047	+0.089 –0.093	+0.133 –0.138	+0.025 –0.028
	18–22	+0.048	+0.056 –0.065	+0.118 –0.125	+0.177 –0.187	+0.038 –0.045
	22–30	+0.060	+0.060 –0.067	+0.126 –0.133	+0.188 –0.198	+0.050 –0.056
	30–50	–0.008	+0.105 –0.117	+0.207 –0.219	+0.303 –0.322	+0.080 –0.094

Table 20: $\lambda_{\vartheta\varphi}$ in the HX frame for the $\psi(2S)$.

$ y $	p_T (GeV)	$\lambda_{\vartheta\varphi}$	Total uncertainty			Stat. unc.
			68.3% CL	95.5% CL	99.7% CL	68.3% CL
0.0–0.6	14–18	−0.030	+0.046 −0.054	+0.095 −0.105	+0.144 −0.154	+0.029 −0.036
	18–22	+0.096	+0.043 −0.048	+0.089 −0.093	+0.134 −0.138	+0.037 −0.040
	22–30	+0.030	+0.047 −0.053	+0.096 −0.102	+0.145 −0.151	+0.041 −0.044
	30–50	−0.007	+0.067 −0.078	+0.141 −0.156	+0.212 −0.234	+0.064 −0.075
0.6–1.2	14–18	+0.046	+0.047 −0.053	+0.096 −0.102	+0.147 −0.151	+0.028 −0.029
	18–22	+0.044	+0.048 −0.053	+0.097 −0.103	+0.147 −0.152	+0.034 −0.037
	22–30	+0.095	+0.048 −0.057	+0.101 −0.110	+0.154 −0.161	+0.038 −0.043
	30–50	−0.037	+0.079 −0.092	+0.160 −0.181	+0.240 −0.266	+0.067 −0.083
1.2–1.5	14–18	+0.005	+0.063 −0.071	+0.132 −0.141	+0.198 −0.210	+0.048 −0.054
	18–22	−0.166	+0.076 −0.090	+0.155 −0.177	+0.233 −0.260	+0.063 −0.080
	22–30	−0.057	+0.081 −0.088	+0.165 −0.172	+0.245 −0.252	+0.069 −0.073
	30–50	+0.019	+0.111 −0.130	+0.231 −0.263	+0.358 −0.397	+0.098 −0.119

Table 21: $\tilde{\lambda}$ in the HX frame for the $\psi(2S)$.

$ y $	p_T (GeV)	$\tilde{\lambda}$	Total uncertainty			Stat. unc.
			68.3% CL	95.5% CL	99.7% CL	68.3% CL
0.0–0.6	14–18	+0.193	+0.226 −0.252	+0.471 −0.485	+0.717 −0.718	+0.171 −0.171
	18–22	+0.133	+0.215 −0.226	+0.448 −0.447	+0.681 −0.657	+0.182 −0.188
	22–30	−0.096	+0.205 −0.203	+0.419 −0.385	+0.633 −0.556	+0.189 −0.178
	30–50	+0.087	+0.329 −0.273	+0.690 −0.530	+1.154 −0.754	+0.320 −0.256
0.6–1.2	14–18	−0.190	+0.171 −0.176	+0.341 −0.345	+0.519 −0.515	+0.132 −0.129
	18–22	−0.329	+0.177 −0.184	+0.353 −0.351	+0.538 −0.508	+0.147 −0.145
	22–30	−0.288	+0.182 −0.180	+0.377 −0.348	+0.572 −0.496	+0.168 −0.161
	30–50	+0.381	+0.361 −0.283	+0.733 −0.537	+1.139 −0.757	+0.347 −0.267
1.2–1.5	14–18	+0.209	+0.230 −0.234	+0.468 −0.460	+0.719 −0.686	+0.201 −0.194
	18–22	+0.326	+0.319 −0.283	+0.642 −0.533	+0.980 −0.767	+0.308 −0.266
	22–30	+0.251	+0.331 −0.281	+0.694 −0.545	+1.075 −0.793	+0.330 −0.275
	30–50	+0.182	+0.492 −0.377	+1.052 −0.742	+1.753 −1.050	+0.474 −0.320

Table 22: λ_θ in the PX frame for the $\psi(2S)$.

$ y $	p_T (GeV)	λ_θ	Total uncertainty			Stat. unc. 68.3% CL
			68.3% CL	95.5% CL	99.7% CL	
0.0–0.6	14–18	+0.256	+0.225 –0.244	+0.459 –0.479	+0.694 –0.701	+0.171 –0.181
	18–22	+0.234	+0.214 –0.228	+0.429 –0.431	+0.656 –0.634	+0.181 –0.185
	22–30	–0.017	+0.185 –0.187	+0.372 –0.355	+0.567 –0.523	+0.164 –0.157
	30–50	+0.070	+0.222 –0.220	+0.460 –0.436	+0.710 –0.651	+0.209 –0.212
0.6–1.2	14–18	–0.078	+0.158 –0.169	+0.317 –0.328	+0.485 –0.487	+0.120 –0.130
	18–22	–0.200	+0.165 –0.175	+0.334 –0.327	+0.504 –0.478	+0.142 –0.145
	22–30	–0.239	+0.159 –0.160	+0.322 –0.308	+0.486 –0.439	+0.141 –0.137
	30–50	+0.298	+0.240 –0.233	+0.482 –0.439	+0.737 –0.633	+0.228 –0.213
1.2–1.5	14–18	+0.144	+0.218 –0.229	+0.448 –0.447	+0.689 –0.665	+0.168 –0.169
	18–22	+0.260	+0.255 –0.249	+0.513 –0.482	+0.783 –0.691	+0.234 –0.227
	22–30	+0.091	+0.239 –0.230	+0.479 –0.447	+0.732 –0.651	+0.224 –0.208
	30–50	+0.212	+0.330 –0.253	+0.677 –0.505	+1.071 –0.710	+0.314 –0.244

Table 23: λ_ϕ in the PX frame for the $\psi(2S)$.

$ y $	p_T (GeV)	λ_ϕ	Total uncertainty			Stat. unc. 68.3% CL
			68.3% CL	95.5% CL	99.7% CL	
0.0–0.6	14–18	–0.022	+0.031 –0.035	+0.063 –0.067	+0.096 –0.101	+0.013 –0.015
	18–22	–0.025	+0.035 –0.039	+0.073 –0.076	+0.110 –0.112	+0.024 –0.025
	22–30	–0.023	+0.037 –0.042	+0.077 –0.082	+0.117 –0.122	+0.030 –0.033
	30–50	+0.011	+0.064 –0.068	+0.131 –0.129	+0.202 –0.190	+0.058 –0.061
0.6–1.2	14–18	–0.038	+0.033 –0.036	+0.068 –0.072	+0.103 –0.107	+0.014 –0.014
	18–22	–0.048	+0.033 –0.037	+0.070 –0.074	+0.105 –0.109	+0.022 –0.023
	22–30	–0.018	+0.045 –0.047	+0.090 –0.093	+0.136 –0.139	+0.031 –0.033
	30–50	+0.033	+0.061 –0.066	+0.129 –0.130	+0.206 –0.193	+0.055 –0.060
1.2–1.5	14–18	+0.019	+0.042 –0.046	+0.086 –0.090	+0.131 –0.135	+0.023 –0.024
	18–22	+0.025	+0.056 –0.062	+0.116 –0.124	+0.175 –0.183	+0.038 –0.042
	22–30	+0.053	+0.060 –0.067	+0.125 –0.128	+0.186 –0.190	+0.049 –0.054
	30–50	–0.006	+0.108 –0.118	+0.213 –0.223	+0.312 –0.328	+0.079 –0.090

Table 24: $\lambda_{\theta\varphi}$ in the PX frame for the $\psi(2S)$.

$ y $	p_T (GeV)	$\lambda_{\theta\varphi}$	Total uncertainty			Stat. unc. 68.3% CL
			68.3% CL	95.5% CL	99.7% CL	
0.0–0.6	14–18	−0.013	+0.043 −0.049	+0.086 −0.095	+0.132 −0.141	+0.028 −0.035
	18–22	+0.108	+0.045 −0.049	+0.090 −0.094	+0.138 −0.139	+0.036 −0.040
	22–30	+0.029	+0.048 −0.054	+0.099 −0.102	+0.149 −0.150	+0.041 −0.045
	30–50	−0.007	+0.071 −0.080	+0.142 −0.154	+0.216 −0.228	+0.063 −0.075
0.6–1.2	14–18	+0.039	+0.045 −0.048	+0.090 −0.096	+0.138 −0.141	+0.026 −0.029
	18–22	+0.024	+0.044 −0.048	+0.088 −0.093	+0.136 −0.136	+0.034 −0.036
	22–30	+0.072	+0.047 −0.053	+0.097 −0.103	+0.144 −0.151	+0.038 −0.043
	30–50	−0.020	+0.080 −0.092	+0.161 −0.177	+0.238 −0.263	+0.068 −0.080
1.2–1.5	14–18	+0.031	+0.060 −0.066	+0.122 −0.127	+0.183 −0.189	+0.047 −0.051
	18–22	−0.145	+0.076 −0.086	+0.153 −0.167	+0.226 −0.244	+0.065 −0.075
	22–30	−0.055	+0.077 −0.085	+0.160 −0.164	+0.239 −0.243	+0.069 −0.074
	30–50	+0.038	+0.111 −0.125	+0.226 −0.259	+0.347 −0.406	+0.098 −0.119

Table 25: $\tilde{\lambda}$ in the PX frame for the $\psi(2S)$.

$ y $	p_T (GeV)	$\tilde{\lambda}$	Total uncertainty			Stat. unc. 68.3% CL
			68.3% CL	95.5% CL	99.7% CL	
0.0–0.6	14–18	+0.185	+0.228 −0.258	+0.478 −0.495	+0.728 −0.732	+0.174 −0.174
	18–22	+0.158	+0.215 −0.234	+0.445 −0.452	+0.675 −0.660	+0.193 −0.192
	22–30	−0.085	+0.205 −0.198	+0.417 −0.378	+0.629 −0.559	+0.190 −0.170
	30–50	+0.084	+0.320 −0.264	+0.681 −0.522	+1.162 −0.745	+0.324 −0.245
0.6–1.2	14–18	−0.185	+0.164 −0.173	+0.338 −0.347	+0.511 −0.511	+0.122 −0.126
	18–22	−0.329	+0.181 −0.188	+0.361 −0.358	+0.550 −0.519	+0.145 −0.144
	22–30	−0.286	+0.186 −0.181	+0.379 −0.355	+0.572 −0.509	+0.168 −0.159
	30–50	+0.385	+0.352 −0.274	+0.717 −0.535	+1.134 −0.760	+0.351 −0.264
1.2–1.5	14–18	+0.204	+0.238 −0.246	+0.493 −0.488	+0.748 −0.717	+0.204 −0.203
	18–22	+0.328	+0.321 −0.277	+0.641 −0.539	+0.977 −0.772	+0.299 −0.269
	22–30	+0.250	+0.343 −0.274	+0.691 −0.543	+1.071 −0.796	+0.337 −0.276
	30–50	+0.184	+0.498 −0.392	+1.047 −0.759	+1.728 −1.047	+0.461 −0.320

B The CMS Collaboration

Yerevan Physics Institute, Yerevan, Armenia

S. Chatrchyan, V. Khachatryan, A.M. Sirunyan, A. Tumasyan

Institut für Hochenergiephysik der OeAW, Wien, Austria

W. Adam, T. Bergauer, M. Dragicevic, J. Erö, C. Fabjan¹, M. Friedl, R. Frühwirth¹, V.M. Ghete, N. Hörmann, J. Hrubec, M. Jeitler¹, W. Kiesenhofer, V. Knünz, M. Krammer¹, I. Krätschmer, D. Liko, I. Mikulec, D. Rabady², B. Rahbaran, C. Rohringer, H. Rohringer, R. Schöfbeck, J. Strauss, A. Taurok, W. Treberer-Treberspurg, W. Waltenberger, C.-E. Wulz¹

National Centre for Particle and High Energy Physics, Minsk, Belarus

V. Mossolov, N. Shumeiko, J. Suarez Gonzalez

Universiteit Antwerpen, Antwerpen, Belgium

S. Alderweireldt, M. Bansal, S. Bansal, T. Cornelis, E.A. De Wolf, X. Janssen, A. Knutsson, S. Luyckx, L. Mucibello, S. Ochesanu, B. Roland, R. Rougny, Z. Staykova, H. Van Haeveermaet, P. Van Mechelen, N. Van Remortel, A. Van Spilbeeck

Vrije Universiteit Brussel, Brussel, Belgium

F. Blekman, S. Blyweert, J. D'Hondt, A. Kalogeropoulos, J. Keaveney, M. Maes, A. Olbrechts, S. Tavernier, W. Van Doninck, P. Van Mulders, G.P. Van Onsem, I. Villella

Université Libre de Bruxelles, Bruxelles, Belgium

C. Caillol, B. Clerboux, G. De Lentdecker, L. Favart, A.P.R. Gay, T. Hreus, A. Léonard, P.E. Marage, A. Mohammadi, L. Perniè, T. Reis, T. Seva, L. Thomas, C. Vander Velde, P. Vanlaer, J. Wang

Ghent University, Ghent, Belgium

V. Adler, K. Beernaert, L. Benucci, A. Cimmino, S. Costantini, S. Dildick, G. Garcia, B. Klein, J. Lellouch, A. Marinov, J. Mccartin, A.A. Ocampo Rios, D. Ryckbosch, M. Sigamani, N. Strobbe, F. Thyssen, M. Tytgat, S. Walsh, E. Yazgan, N. Zaganidis

Université Catholique de Louvain, Louvain-la-Neuve, Belgium

S. Basegmez, C. Beluffi³, G. Bruno, R. Castello, A. Caudron, L. Ceard, G.G. Da Silva, C. Delaere, T. du Pree, D. Favart, L. Forthomme, A. Giammanco⁴, J. Hollar, P. Jez, V. Lemaitre, J. Liao, O. Militaru, C. Nuttens, D. Pagano, A. Pin, K. Piotrkowski, A. Popov⁵, M. Selvaggi, J.M. Vizan Garcia

Université de Mons, Mons, Belgium

N. Bely, T. Caebergs, E. Daubie, G.H. Hammad

Centro Brasileiro de Pesquisas Fisicas, Rio de Janeiro, Brazil

G.A. Alves, M. Correa Martins Junior, T. Martins, M.E. Pol, M.H.G. Souza

Universidade do Estado do Rio de Janeiro, Rio de Janeiro, Brazil

W.L. Aldá Júnior, W. Carvalho, J. Chinellato⁶, A. Custódio, E.M. Da Costa, D. De Jesus Damiao, C. De Oliveira Martins, S. Fonseca De Souza, H. Malbouisson, M. Malek, D. Matos Figueiredo, L. Mundim, H. Nogima, W.L. Prado Da Silva, A. Santoro, A. Sznajder, E.J. Tonelli Manganote⁶, A. Vilela Pereira

Universidade Estadual Paulista ^a, Universidade Federal do ABC ^b, São Paulo, Brazil

C.A. Bernardes^b, F.A. Dias^{a,7}, T.R. Fernandez Perez Tomei^a, E.M. Gregores^b, C. Lagana^a, P.G. Mercadante^b, S.F. Novaes^a, Sandra S. Padula^a

Institute for Nuclear Research and Nuclear Energy, Sofia, Bulgaria

V. Genchev², P. Iaydjiev², S. Piperov, M. Rodozov, G. Sultanov, M. Vutova

University of Sofia, Sofia, Bulgaria

A. Dimitrov, R. Hadjiiska, V. Kozhuharov, L. Litov, B. Pavlov, P. Petkov

Institute of High Energy Physics, Beijing, China

J.G. Bian, G.M. Chen, H.S. Chen, C.H. Jiang, D. Liang, S. Liang, X. Meng, J. Tao, X. Wang, Z. Wang, H. Xiao

State Key Laboratory of Nuclear Physics and Technology, Peking University, Beijing, China

C. Asawatrangkuldee, Y. Ban, Y. Guo, W. Li, S. Liu, Y. Mao, S.J. Qian, H. Teng, D. Wang, L. Zhang, W. Zou

Universidad de Los Andes, Bogota, Colombia

C. Avila, C.A. Carrillo Montoya, L.F. Chaparro Sierra, J.P. Gomez, B. Gomez Moreno, J.C. Sanabria

Technical University of Split, Split, Croatia

N. Godinovic, D. Lelas, R. Plestina⁸, D. Polic, I. Puljak

University of Split, Split, Croatia

Z. Antunovic, M. Kovac

Institute Rudjer Boskovic, Zagreb, Croatia

V. Brigljevic, K. Kadija, J. Luetic, D. Mekterovic, S. Morovic, L. Tikvica

University of Cyprus, Nicosia, Cyprus

A. Attikis, G. Mavromanolakis, J. Mousa, C. Nicolaou, F. Ptochos, P.A. Razis

Charles University, Prague, Czech Republic

M. Finger, M. Finger Jr.

Academy of Scientific Research and Technology of the Arab Republic of Egypt, Egyptian Network of High Energy Physics, Cairo, Egypt

Y. Assran⁹, S. Elgammal¹⁰, A. Ellithi Kamel¹¹, A.M. Kuotb Awad¹², M.A. Mahmoud¹², A. Radi^{13,14}

National Institute of Chemical Physics and Biophysics, Tallinn, Estonia

M. Kadastik, M. Müntel, M. Murumaa, M. Raidal, L. Rebane, A. Tiko

Department of Physics, University of Helsinki, Helsinki, Finland

P. Eerola, G. Fedi, M. Voutilainen

Helsinki Institute of Physics, Helsinki, Finland

J. Härkönen, V. Karimäki, R. Kinnunen, M.J. Kortelainen, T. Lampén, K. Lassila-Perini, S. Lehti, T. Lindén, P. Luukka, T. Mäenpää, T. Peltola, E. Tuominen, J. Tuominiemi, E. Tuovinen, L. Wendland

Lappeenranta University of Technology, Lappeenranta, Finland

T. Tuuva

DSM/IRFU, CEA/Saclay, Gif-sur-Yvette, France

M. Besancon, F. Couderc, M. Dejardin, D. Denegri, B. Fabbro, J.L. Faure, F. Ferri, S. Ganjour, A. Givernaud, P. Gras, G. Hamel de Monchenault, P. Jarry, E. Locci, J. Malcles, L. Millischer, A. Nayak, J. Rander, A. Rosowsky, M. Titov

Laboratoire Leprince-Ringuet, Ecole Polytechnique, IN2P3-CNRS, Palaiseau, France

S. Baffioni, F. Beaudette, L. Benhabib, M. Bluj¹⁵, P. Busson, C. Charlot, N. Daci, T. Dahms, M. Dalchenko, L. Dobrzynski, A. Florent, R. Granier de Cassagnac, M. Haguenaer, P. Miné, C. Mironov, I.N. Naranjo, M. Nguyen, C. Ochando, P. Paganini, D. Sabes, R. Salerno, Y. Sirois, C. Veelken, A. Zabi

Institut Pluridisciplinaire Hubert Curien, Université de Strasbourg, Université de Haute Alsace Mulhouse, CNRS/IN2P3, Strasbourg, France

J.-L. Agram¹⁶, J. Andrea, D. Bloch, J.-M. Brom, E.C. Chabert, C. Collard, E. Conte¹⁶, F. Drouhin¹⁶, J.-C. Fontaine¹⁶, D. Gelé, U. Goerlach, C. Goetzmann, P. Juillot, A.-C. Le Bihan, P. Van Hove

Centre de Calcul de l'Institut National de Physique Nucleaire et de Physique des Particules, CNRS/IN2P3, Villeurbanne, France

S. Gadrat

Université de Lyon, Université Claude Bernard Lyon 1, CNRS-IN2P3, Institut de Physique Nucléaire de Lyon, Villeurbanne, France

S. Beauceron, N. Beaupere, G. Boudoul, S. Brochet, J. Chasserat, R. Chierici, D. Contardo, P. Depasse, H. El Mamouni, J. Fay, S. Gascon, M. Gouzevitch, B. Ille, T. Kurca, M. Lethuillier, L. Mirabito, S. Perries, L. Sgandurra, V. Sordini, M. Vander Donckt, P. Verdier, S. Viret

Institute of High Energy Physics and Informatization, Tbilisi State University, Tbilisi, Georgia

Z. Tsamalaidze¹⁷

RWTH Aachen University, I. Physikalisches Institut, Aachen, Germany

C. Autermann, S. Beranek, B. Calpas, M. Edelhoff, L. Feld, N. Heracleous, O. Hindrichs, K. Klein, A. Ostapchuk, A. Perieanu, F. Raupach, J. Sammet, S. Schael, D. Sprenger, H. Weber, B. Wittmer, V. Zhukov⁵

RWTH Aachen University, III. Physikalisches Institut A, Aachen, Germany

M. Ata, J. Caudron, E. Dietz-Laursonn, D. Duchardt, M. Erdmann, R. Fischer, A. Güth, T. Hebbeker, C. Heidemann, K. Hoepfner, D. Klingebiel, S. Knutzen, P. Kreuzer, M. Merschmeyer, A. Meyer, M. Olschewski, K. Padeken, P. Papacz, H. Pieta, H. Reithler, S.A. Schmitz, L. Sonnenschein, J. Steggemann, D. Teyssier, S. Thüer, M. Weber

RWTH Aachen University, III. Physikalisches Institut B, Aachen, Germany

V. Cherepanov, Y. Erdogan, G. Flügge, H. Geenen, M. Geisler, W. Haj Ahmad, F. Hoehle, B. Kargoll, T. Kress, Y. Kuessel, J. Lingemann², A. Nowack, I.M. Nugent, L. Perchalla, O. Pooth, A. Stahl

Deutsches Elektronen-Synchrotron, Hamburg, Germany

I. Asin, N. Bartosik, J. Behr, W. Behrenhoff, U. Behrens, A.J. Bell, M. Bergholz¹⁸, A. Bethani, K. Borras, A. Burgmeier, A. Cakir, L. Calligaris, A. Campbell, S. Choudhury, F. Costanza, C. Diez Pardos, S. Dooling, T. Dorland, G. Eckerlin, D. Eckstein, G. Flucke, A. Geiser, I. Glushkov, A. Grebenyuk, P. Gunnellini, S. Habib, J. Hauk, G. Hellwig, D. Horton, H. Jung, M. Kasemann, P. Katsas, C. Kleinwort, H. Kluge, M. Krämer, D. Krücker, E. Kuznetsova, W. Lange, J. Leonard, K. Lipka, W. Lohmann¹⁸, B. Lutz, R. Mankel, I. Marfin, I.-A. Melzer-Pellmann, A.B. Meyer, J. Mnich, A. Mussgiller, S. Naumann-Emme, O. Novgorodova, F. Nowak, J. Olzem, H. Perrey, A. Petrukhin, D. Pitzl, R. Placakyte, A. Raspereza, P.M. Ribeiro Cipriano, C. Riedl, E. Ron, M.Ö. Sahin, J. Salfeld-Nebgen, R. Schmidt¹⁸, T. Schoerner-Sadenius, N. Sen, M. Stein, R. Walsh, C. Wissing

University of Hamburg, Hamburg, Germany

M. Aldaya Martin, V. Blobel, H. Enderle, J. Erfle, E. Garutti, U. Gebbert, M. Görner, M. Gosselink, J. Haller, K. Heine, R.S. Höing, G. Kaussen, H. Kirschenmann, R. Klanner, R. Kogler, J. Lange, I. Marchesini, T. Peiffer, N. Pietsch, D. Rathjens, C. Sander, H. Schettler, P. Schleper, E. Schlieckau, A. Schmidt, M. Schröder, T. Schum, M. Seidel, J. Sibille¹⁹, V. Sola, H. Stadie, G. Steinbrück, J. Thomsen, D. Troendle, E. Usai, L. Vanelderen

Institut für Experimentelle Kernphysik, Karlsruhe, Germany

C. Barth, C. Baus, J. Berger, C. Böser, E. Butz, T. Chwalek, W. De Boer, A. Descroix, A. Dierlamm, M. Feindt, M. Guthoff², F. Hartmann², T. Hauth², H. Held, K.H. Hoffmann, U. Husemann, I. Katkov⁵, J.R. Komaragiri, A. Kornmayer², P. Lobelle Pardo, D. Martschei, Th. Müller, M. Niegel, A. Nürnberg, O. Oberst, J. Ott, G. Quast, K. Rabbertz, F. Ratnikov, S. Röcker, F.-P. Schilling, G. Schott, H.J. Simonis, F.M. Stober, R. Ulrich, J. Wagner-Kuhr, S. Wayand, T. Weiler, M. Zeise

Institute of Nuclear and Particle Physics (INPP), NCSR Demokritos, Aghia Paraskevi, Greece

G. Anagnostou, G. Daskalakis, T. Geralis, S. Kesisoglou, A. Kyriakis, D. Loukas, A. Markou, C. Markou, E. Ntomari, I. Topsis-giotis

University of Athens, Athens, Greece

L. Gouskos, A. Panagiotou, N. Saoulidou, E. Stiliaris

University of Ioánnina, Ioánnina, Greece

X. Aslanoglou, I. Evangelou, G. Flouris, C. Foudas, P. Kokkas, N. Manthos, I. Papadopoulos, E. Paradas

KFKI Research Institute for Particle and Nuclear Physics, Budapest, Hungary

G. Bencze, C. Hajdu, P. Hidas, D. Horvath²⁰, F. Sikler, V. Veszpremi, G. Vesztergombi²¹, A.J. Zsigmond

Institute of Nuclear Research ATOMKI, Debrecen, Hungary

N. Beni, S. Czellar, J. Molnar, J. Palinkas, Z. Szillasi

University of Debrecen, Debrecen, Hungary

J. Karacsi, P. Raics, Z.L. Trocsanyi, B. Ujvari

National Institute of Science Education and Research, Bhubaneswar, India

S.K. Swain²²

Panjab University, Chandigarh, India

S.B. Beri, V. Bhatnagar, N. Dhingra, R. Gupta, M. Kaur, M.Z. Mehta, M. Mittal, N. Nishu, A. Sharma, J.B. Singh

University of Delhi, Delhi, India

Ashok Kumar, Arun Kumar, S. Ahuja, A. Bhardwaj, B.C. Choudhary, S. Malhotra, M. Naimuddin, K. Ranjan, P. Saxena, V. Sharma, R.K. Shivpuri

Saha Institute of Nuclear Physics, Kolkata, India

S. Banerjee, S. Bhattacharya, K. Chatterjee, S. Dutta, B. Gomber, Sa. Jain, Sh. Jain, R. Khurana, A. Modak, S. Mukherjee, D. Roy, S. Sarkar, M. Sharan, A.P. Singh

Bhabha Atomic Research Centre, Mumbai, India

A. Abdulsalam, D. Dutta, S. Kailas, V. Kumar, A.K. Mohanty², L.M. Pant, P. Shukla, A. Topkar

Tata Institute of Fundamental Research - EHEP, Mumbai, India

T. Aziz, R.M. Chatterjee, S. Ganguly, S. Ghosh, M. Guchait²³, A. Gurtu²⁴, G. Kole, S. Kumar, M. Maity²⁵, G. Majumder, K. Mazumdar, G.B. Mohanty, B. Parida, K. Sudhakar, N. Wickramage²⁶

Tata Institute of Fundamental Research - HECR, Mumbai, India

S. Banerjee, S. Dugad

Institute for Research in Fundamental Sciences (IPM), Tehran, Iran

H. Arfaei, H. Bakhshiansohi, S.M. Etesami²⁷, A. Fahim²⁸, A. Jafari, M. Khakzad, M. Mohammadi Najafabadi, S. Paktinat Mehdiabadi, B. Safarzadeh²⁹, M. Zeinali

University College Dublin, Dublin, Ireland

M. Grunewald

INFN Sezione di Bari ^a, Università di Bari ^b, Politecnico di Bari ^c, Bari, Italy

M. Abbrescia^{a,b}, L. Barbone^{a,b}, C. Calabria^{a,b}, S.S. Chhibra^{a,b}, A. Colaleo^a, D. Creanza^{a,c}, N. De Filippis^{a,c}, M. De Palma^{a,b}, L. Fiore^a, G. Iaselli^{a,c}, G. Maggi^{a,c}, M. Maggi^a, B. Marangelli^{a,b}, S. My^{a,c}, S. Nuzzo^{a,b}, N. Pacifico^a, A. Pompili^{a,b}, G. Pugliese^{a,c}, G. Selvaggi^{a,b}, L. Silvestris^a, G. Singh^{a,b}, R. Venditti^{a,b}, P. Verwilligen^a, G. Zito^a

INFN Sezione di Bologna ^a, Università di Bologna ^b, Bologna, Italy

G. Abbiendi^a, A.C. Benvenuti^a, D. Bonacorsi^{a,b}, S. Braibant-Giacomelli^{a,b}, L. Brigliadori^{a,b}, R. Campanini^{a,b}, P. Capiluppi^{a,b}, A. Castro^{a,b}, F.R. Cavallo^a, G. Codispoti^{a,b}, M. Cuffiani^{a,b}, G.M. Dallavalle^a, F. Fabbri^a, A. Fanfani^{a,b}, D. Fasanella^{a,b}, P. Giacomelli^a, C. Grandi^a, L. Guiducci^{a,b}, S. Marcellini^a, G. Masetti^a, M. Meneghelli^{a,b}, A. Montanari^a, F.L. Navarria^{a,b}, F. Odorici^a, A. Perrotta^a, F. Primavera^{a,b}, A.M. Rossi^{a,b}, T. Rovelli^{a,b}, G.P. Siroli^{a,b}, N. Tosi^{a,b}, R. Travaglini^{a,b}

INFN Sezione di Catania ^a, Università di Catania ^b, Catania, Italy

S. Albergo^{a,b}, M. Chiorboli^{a,b}, S. Costa^{a,b}, F. Giordano^{a,2}, R. Potenza^{a,b}, A. Tricomi^{a,b}, C. Tuve^{a,b}

INFN Sezione di Firenze ^a, Università di Firenze ^b, Firenze, Italy

G. Barbagli^a, V. Ciulli^{a,b}, C. Civinini^a, R. D'Alessandro^{a,b}, E. Focardi^{a,b}, S. Frosali^{a,b}, E. Gallo^a, S. Gonzi^{a,b}, V. Gori^{a,b}, P. Lenzi^{a,b}, M. Meschini^a, S. Paoletti^a, G. Sguazzoni^a, A. Tropiano^{a,b}

INFN Laboratori Nazionali di Frascati, Frascati, Italy

L. Benussi, S. Bianco, F. Fabbri, D. Piccolo

INFN Sezione di Genova ^a, Università di Genova ^b, Genova, Italy

P. Fabbricatore^a, R. Ferretti^{a,b}, F. Ferro^a, M. Lo Vetere^{a,b}, R. Musenich^a, E. Robutti^a, S. Tosi^{a,b}

INFN Sezione di Milano-Bicocca ^a, Università di Milano-Bicocca ^b, Milano, Italy

A. Benaglia^a, M.E. Dinardo^{a,b}, S. Fiorendi^{a,b}, S. Gennai^a, A. Ghezzi^{a,b}, P. Govoni^{a,b}, M.T. Lucchini^{a,b,2}, S. Malvezzi^a, R.A. Manzoni^{a,b,2}, A. Martelli^{a,b,2}, D. Menasce^a, L. Moroni^a, M. Paganoni^{a,b}, D. Pedrini^a, S. Ragazzi^{a,b}, N. Redaelli^a, T. Tabarelli de Fatis^{a,b}

INFN Sezione di Napoli ^a, Università di Napoli 'Federico II' ^b, Università della Basilicata (Potenza) ^c, Università G. Marconi (Roma) ^d, Napoli, Italy

S. Buontempo^a, N. Cavallo^{a,c}, A. De Cosa^{a,b}, F. Fabozzi^{a,c}, A.O.M. Iorio^{a,b}, L. Lista^a, S. Meola^{a,d,2}, M. Merola^a, P. Paolucci^{a,2}

INFN Sezione di Padova ^a, Università di Padova ^b, Università di Trento (Trento) ^c, Padova, Italy

P. Azzi^a, N. Bacchetta^a, M. Biasotto^{a,30}, D. Bisello^{a,b}, A. Branca^{a,b}, R. Carlin^{a,b}, P. Checchia^a,

T. Dorigo^a, M. Galanti^{a,b,2}, F. Gasparini^{a,b}, U. Gasparini^{a,b}, P. Giubilato^{a,b}, A. Gozzelino^a, K. Kanishchev^{a,c}, S. Lacaprara^a, I. Lazzizzera^{a,c}, M. Margoni^{a,b}, A.T. Meneguzzo^{a,b}, M. Passaseo^a, J. Pazzini^{a,b}, N. Pozzobon^{a,b}, P. Ronchese^{a,b}, F. Simonetto^{a,b}, E. Torassa^a, M. Tosi^{a,b}, A. Triossi^a, S. Vanini^{a,b}, S. Ventura^a, P. Zotto^{a,b}, A. Zucchetta^{a,b}, G. Zumerle^{a,b}

INFN Sezione di Pavia^a, Università di Pavia^b, Pavia, Italy

M. Gabusi^{a,b}, S.P. Ratti^{a,b}, C. Riccardi^{a,b}, P. Vitulo^{a,b}

INFN Sezione di Perugia^a, Università di Perugia^b, Perugia, Italy

M. Biasini^{a,b}, G.M. Bilei^a, L. Fanò^{a,b}, P. Lariccia^{a,b}, G. Mantovani^{a,b}, M. Menichelli^a, A. Nappi^{a,b†}, F. Romeo^{a,b}, A. Saha^a, A. Santocchia^{a,b}, A. Spiezia^{a,b}

INFN Sezione di Pisa^a, Università di Pisa^b, Scuola Normale Superiore di Pisa^c, Pisa, Italy

K. Androsov^{a,31}, P. Azzurri^a, G. Bagliesi^a, T. Boccali^a, G. Broccolo^{a,c}, R. Castaldi^a, M.A. Ciocci^a, R.T. D'Agnolo^{a,c,2}, R. Dell'Orso^a, F. Fiori^{a,c}, L. Foà^{a,c}, A. Giassi^a, M.T. Grippo^{a,31}, A. Kraan^a, F. Ligabue^{a,c}, T. Lomtadze^a, L. Martini^{a,31}, A. Messineo^{a,b}, C.S. Moon^a, F. Palla^a, A. Rizzi^{a,b}, A. Savoy-Navarro^{a,32}, A.T. Serban^a, P. Spagnolo^a, P. Squillacioti^a, R. Tenchini^a, G. Tonelli^{a,b}, A. Venturi^a, P.G. Verdini^a, C. Vernieri^{a,c}

INFN Sezione di Roma^a, Università di Roma^b, Roma, Italy

L. Barone^{a,b}, F. Cavallari^a, D. Del Re^{a,b}, M. Diemoz^a, M. Grassi^{a,b}, E. Longo^{a,b}, F. Margaroli^{a,b}, P. Meridiani^a, F. Micheli^{a,b}, S. Nourbakhsh^{a,b}, G. Organtini^{a,b}, R. Paramatti^a, S. Rahatlou^{a,b}, C. Rovelli^a, L. Soffi^{a,b}

INFN Sezione di Torino^a, Università di Torino^b, Università del Piemonte Orientale (Novara)^c, Torino, Italy

N. Amapane^{a,b}, R. Arcidiacono^{a,c}, S. Argiro^{a,b}, M. Arneodo^{a,c}, R. Bellan^{a,b}, C. Biino^a, N. Cartiglia^a, S. Casasso^{a,b}, M. Costa^{a,b}, A. Degano^{a,b}, N. Demaria^a, C. Mariotti^a, S. Maselli^a, E. Migliore^{a,b}, V. Monaco^{a,b}, M. Musich^a, M.M. Obertino^{a,c}, N. Pastrone^a, M. Pelliccioni^{a,2}, A. Potenza^{a,b}, A. Romero^{a,b}, M. Ruspa^{a,c}, R. Sacchi^{a,b}, A. Solano^{a,b}, A. Staiano^a, U. Tamponi^a

INFN Sezione di Trieste^a, Università di Trieste^b, Trieste, Italy

S. Belforte^a, V. Candelise^{a,b}, M. Casarsa^a, F. Cossutti^{a,2}, G. Della Ricca^{a,b}, B. Gobbo^a, C. La Licata^{a,b}, M. Marone^{a,b}, D. Montanino^{a,b}, A. Penzo^a, A. Schizzi^{a,b}, A. Zanetti^a

Kangwon National University, Chunchon, Korea

S. Chang, T.Y. Kim, S.K. Nam

Kyungpook National University, Daegu, Korea

D.H. Kim, G.N. Kim, J.E. Kim, D.J. Kong, S. Lee, Y.D. Oh, H. Park, D.C. Son

Chonnam National University, Institute for Universe and Elementary Particles, Kwangju, Korea

J.Y. Kim, Zero J. Kim, S. Song

Korea University, Seoul, Korea

S. Choi, D. Gyun, B. Hong, M. Jo, H. Kim, T.J. Kim, K.S. Lee, S.K. Park, Y. Roh

University of Seoul, Seoul, Korea

M. Choi, J.H. Kim, C. Park, I.C. Park, S. Park, G. Ryu

Sungkyunkwan University, Suwon, Korea

Y. Choi, Y.K. Choi, J. Goh, M.S. Kim, E. Kwon, B. Lee, J. Lee, S. Lee, H. Seo, I. Yu

Vilnius University, Vilnius, Lithuania

I. Grigelionis, A. Juodagalvis

Centro de Investigacion y de Estudios Avanzados del IPN, Mexico City, Mexico

H. Castilla-Valdez, E. De La Cruz-Burelo, I. Heredia-de La Cruz³³, R. Lopez-Fernandez, J. Martínez-Ortega, A. Sanchez-Hernandez, L.M. Villasenor-Cendejas

Universidad Iberoamericana, Mexico City, Mexico

S. Carrillo Moreno, F. Vazquez Valencia

Benemerita Universidad Autonoma de Puebla, Puebla, Mexico

H.A. Salazar Ibarquen

Universidad Autónoma de San Luis Potosí, San Luis Potosí, Mexico

E. Casimiro Linares, A. Morelos Pineda, M.A. Reyes-Santos

University of Auckland, Auckland, New Zealand

D. Krofcheck

University of Canterbury, Christchurch, New Zealand

P.H. Butler, R. Doesburg, S. Reucroft, H. Silverwood

National Centre for Physics, Quaid-I-Azam University, Islamabad, Pakistan

M. Ahmad, M.I. Asghar, J. Butt, H.R. Hoorani, S. Khalid, W.A. Khan, T. Khurshid, S. Qazi, M.A. Shah, M. Shoaib

National Centre for Nuclear Research, Swierk, Poland

H. Bialkowska, B. Boimska, T. Frueboes, M. Górski, M. Kazana, K. Nawrocki, K. Romanowska-Rybinska, M. Szleper, G. Wrochna, P. Zalewski

Institute of Experimental Physics, Faculty of Physics, University of Warsaw, Warsaw, Poland

G. Brona, K. Bunkowski, M. Cwiok, W. Dominik, K. Doroba, A. Kalinowski, M. Konecki, J. Krolikowski, M. Misiura

Laboratório de Instrumentação e Física Experimental de Partículas, Lisboa, Portugal

N. Almeida, P. Bargassa, C. Beirão Da Cruz E Silva, P. Faccioli, P.G. Ferreira Parracho, M. Gallinaro, F. Nguyen, J. Rodrigues Antunes, J. Seixas², J. Varela, P. Vischia

Joint Institute for Nuclear Research, Dubna, Russia

S. Afanasiev, P. Bunin, M. Gavrilenko, I. Golutvin, I. Gorbunov, A. Kamenev, V. Karjavin, V. Konoplyanikov, A. Lanev, A. Malakhov, V. Matveev, P. Moisezenz, V. Palichik, V. Perelygin, S. Shmatov, N. Skatchkov, V. Smirnov, A. Zarubin

Petersburg Nuclear Physics Institute, Gatchina (St. Petersburg), Russia

S. Evstyukhin, V. Golovtsov, Y. Ivanov, V. Kim, P. Levchenko, V. Murzin, V. Oreshkin, I. Smirnov, V. Sulimov, L. Uvarov, S. Vavilov, A. Vorobyev, An. Vorobyev

Institute for Nuclear Research, Moscow, Russia

Yu. Andreev, A. Dermenev, S. Gninenko, N. Golubev, M. Kirsanov, N. Krasnikov, A. Pashenkov, D. Tlisov, A. Toropin

Institute for Theoretical and Experimental Physics, Moscow, Russia

V. Epshteyn, M. Erofeeva, V. Gavrilov, N. Lychkovskaya, V. Popov, G. Safronov, S. Semenov, A. Spiridonov, V. Stolin, E. Vlasov, A. Zhokin

P.N. Lebedev Physical Institute, Moscow, Russia

V. Andreev, M. Azarkin, I. Dremin, M. Kirakosyan, A. Leonidov, G. Mesyats, S.V. Rusakov, A. Vinogradov

Skobeltsyn Institute of Nuclear Physics, Lomonosov Moscow State University, Moscow, Russia

A. Belyaev, E. Boos, M. Dubinin⁷, L. Dudko, A. Ershov, A. Gribushin, V. Klyukhin, O. Kodolova, I. Lokhtin, A. Markina, S. Obraztsov, S. Petrushanko, V. Savrin, A. Snigirev

State Research Center of Russian Federation, Institute for High Energy Physics, Protvino, Russia

I. Azhgirey, I. Bayshev, S. Bitioukov, V. Kachanov, A. Kalinin, D. Konstantinov, V. Krychkin, V. Petrov, R. Ryutin, A. Sobol, L. Tourtchanovitch, S. Troshin, N. Tyurin, A. Uzunian, A. Volkov

University of Belgrade, Faculty of Physics and Vinca Institute of Nuclear Sciences, Belgrade, Serbia

P. Adzic³⁴, M. Djordjevic, M. Ekmedzic, D. Krpic³⁴, J. Milosevic

Centro de Investigaciones Energéticas Medioambientales y Tecnológicas (CIEMAT), Madrid, Spain

M. Aguilar-Benitez, J. Alcaraz Maestre, C. Battilana, E. Calvo, M. Cerrada, M. Chamizo Llatas², N. Colino, B. De La Cruz, A. Delgado Peris, D. Domínguez Vázquez, C. Fernandez Bedoya, J.P. Fernández Ramos, A. Ferrando, J. Flix, M.C. Fouz, P. Garcia-Abia, O. Gonzalez Lopez, S. Goy Lopez, J.M. Hernandez, M.I. Josa, G. Merino, E. Navarro De Martino, J. Puerta Pelayo, A. Quintario Olmeda, I. Redondo, L. Romero, J. Santaolalla, M.S. Soares, C. Willmott

Universidad Autónoma de Madrid, Madrid, Spain

C. Albajar, J.F. de Trocóniz

Universidad de Oviedo, Oviedo, Spain

H. Brun, J. Cuevas, J. Fernandez Menendez, S. Folgueras, I. Gonzalez Caballero, L. Lloret Iglesias, J. Piedra Gomez

Instituto de Física de Cantabria (IFCA), CSIC-Universidad de Cantabria, Santander, Spain

J.A. Brochero Cifuentes, I.J. Cabrillo, A. Calderon, S.H. Chuang, J. Duarte Campderros, M. Fernandez, G. Gomez, J. Gonzalez Sanchez, A. Graziano, C. Jorda, A. Lopez Virto, J. Marco, R. Marco, C. Martinez Rivero, F. Matorras, F.J. Munoz Sanchez, T. Rodrigo, A.Y. Rodríguez-Marrero, A. Ruiz-Jimeno, L. Scodellaro, I. Vila, R. Vilar Cortabitarte

CERN, European Organization for Nuclear Research, Geneva, Switzerland

D. Abbaneo, E. Auffray, G. Auzinger, M. Bachtis, P. Baillon, A.H. Ball, D. Barney, J. Bendavid, J.F. Benitez, C. Bernet⁸, G. Bianchi, P. Bloch, A. Bocci, A. Bonato, O. Bondu, C. Botta, H. Breuker, T. Camporesi, G. Cerminara, T. Christiansen, J.A. Coarasa Perez, S. Colafranceschi³⁵, M. D'Alfonso, D. d'Enterria, A. Dabrowski, A. David, F. De Guio, A. De Roeck, S. De Visscher, S. Di Guida, M. Dobson, N. Dupont-Sagorin, A. Elliott-Peisert, J. Eugster, W. Funk, G. Georgiou, M. Giffels, D. Gigi, K. Gill, D. Giordano, M. Girone, M. Giunta, F. Glege, R. Gomez-Reino Garrido, S. Gowdy, R. Guida, J. Hammer, M. Hansen, P. Harris, C. Hartl, A. Hinzmann, V. Innocente, P. Janot, E. Karavakis, K. Kousouris, K. Krajczar, P. Lecoq, Y.-J. Lee, C. Lourenço, N. Magini, L. Malgeri, M. Mannelli, L. Masetti, F. Meijers, S. Mersi, E. Meschi, R. Moser, M. Mulders, P. Musella, E. Nesvold, L. Orsini, E. Palencia Cortezon, E. Perez, L. Perrozzi, A. Petrilli, A. Pfeiffer, M. Pierini, M. Pimiä, D. Piparo, M. Plagge, L. Quertenmont, A. Racz, W. Reece, G. Rolandi³⁶, M. Rovere, H. Sakulin, F. Santanastasio, C. Schäfer, C. Schwick, I. Segoni, S. Sekmen, A. Sharma, P. Siegrist, P. Silva, M. Simon, P. Sphicas³⁷, D. Spiga, M. Stoye, A. Tsiros, G.I. Veres²¹, J.R. Vlimant, H.K. Wöhri, S.D. Worm³⁸, W.D. Zeuner

Paul Scherrer Institut, Villigen, Switzerland

W. Bertl, K. Deiters, W. Erdmann, K. Gabathuler, R. Horisberger, Q. Ingram, H.C. Kaestli, S. König, D. Kotlinski, U. Langenegger, D. Renker, T. Rohe

Institute for Particle Physics, ETH Zurich, Zurich, Switzerland

F. Bachmair, L. Bäni, L. Bianchini, P. Bortignon, M.A. Buchmann, B. Casal, N. Chanon, A. Deisher, G. Dissertori, M. Dittmar, M. Donegà, M. Dünser, P. Eller, K. Freudenreich, C. Grab, D. Hits, P. Lecomte, W. Lustermann, B. Mangano, A.C. Marini, P. Martinez Ruiz del Arbol, D. Meister, N. Mohr, F. Moortgat, C. Nägeli³⁹, P. Nef, F. Nessi-Tedaldi, F. Pandolfi, L. Pape, F. Pauss, M. Peruzzi, F.J. Ronga, M. Rossini, L. Sala, A.K. Sanchez, A. Starodumov⁴⁰, B. Stieger, M. Takahashi, L. Tauscher[†], A. Thea, K. Theofilatos, D. Treille, C. Urscheler, R. Wallny, H.A. Weber

Universität Zürich, Zurich, Switzerland

C. Amsler⁴¹, V. Chiochia, C. Favaro, M. Ivova Rikova, B. Kilminster, B. Millan Mejias, P. Robmann, H. Snoek, S. Taroni, M. Verzetti, Y. Yang

National Central University, Chung-Li, Taiwan

M. Cardaci, K.H. Chen, C. Ferro, C.M. Kuo, S.W. Li, W. Lin, Y.J. Lu, R. Volpe, S.S. Yu

National Taiwan University (NTU), Taipei, Taiwan

P. Bartalini, P. Chang, Y.H. Chang, Y.W. Chang, Y. Chao, K.F. Chen, C. Dietz, U. Grundler, W.-S. Hou, Y. Hsiung, K.Y. Kao, Y.J. Lei, R.-S. Lu, D. Majumder, E. Petrakou, X. Shi, J.G. Shiu, Y.M. Tzeng, M. Wang

Chulalongkorn University, Bangkok, Thailand

B. Asavapibhop, N. Suwonjandee

Cukurova University, Adana, Turkey

A. Adiguzel, M.N. Bakirci⁴², S. Cerci⁴³, C. Dozen, I. Dumanoglu, E. Eskut, S. Girgis, G. Gokbulut, E. Gurpinar, I. Hos, E.E. Kangal, A. Kayis Topaksu, G. Onengut⁴⁴, K. Ozdemir, S. Ozturk⁴², A. Polatoz, K. Sogut⁴⁵, D. Sunar Cerci⁴³, B. Tali⁴³, H. Topakli⁴², M. Vergili

Middle East Technical University, Physics Department, Ankara, Turkey

I.V. Akin, T. Aliev, B. Bilin, S. Bilmis, M. Deniz, H. Gamsizkan, A.M. Guler, G. Karapinar⁴⁶, K. Ocalan, A. Ozpineci, M. Serin, R. Sever, U.E. Surat, M. Yalvac, M. Zeyrek

Bogazici University, Istanbul, Turkey

E. Gülmez, B. Isildak⁴⁷, M. Kaya⁴⁸, O. Kaya⁴⁸, S. Ozkorucuklu⁴⁹, N. Sonmez⁵⁰

Istanbul Technical University, Istanbul, Turkey

H. Bahtiyar⁵¹, E. Barlas, K. Cankocak, Y.O. Günaydin⁵², F.I. Vardarli, M. Yücel

National Scientific Center, Kharkov Institute of Physics and Technology, Kharkov, Ukraine

L. Levchuk, P. Sorokin

University of Bristol, Bristol, United Kingdom

J.J. Brooke, E. Clement, D. Cussans, H. Flacher, R. Frazier, J. Goldstein, M. Grimes, G.P. Heath, H.F. Heath, L. Kreczko, C. Lucas, Z. Meng, S. Metson, D.M. Newbold³⁸, K. Nirunpong, S. Paramesvaran, A. Poll, S. Senkin, V.J. Smith, T. Williams

Rutherford Appleton Laboratory, Didcot, United Kingdom

K.W. Bell, A. Belyaev⁵³, C. Brew, R.M. Brown, D.J.A. Cockerill, J.A. Coughlan, K. Harder, S. Harper, E. Olaiya, D. Petyt, B.C. Radburn-Smith, C.H. Shepherd-Themistocleous, I.R. Tomalin, W.J. Womersley

Imperial College, London, United Kingdom

R. Bainbridge, O. Buchmuller, D. Burton, D. Colling, N. Cripps, M. Cutajar, P. Dauncey, G. Davies, M. Della Negra, W. Ferguson, J. Fulcher, D. Futyan, A. Gilbert, A. Guneratne Bryer, G. Hall, Z. Hatherell, J. Hays, G. Iles, M. Jarvis, G. Karapostoli, M. Kenzie, R. Lane, R. Lucas³⁸, L. Lyons, A.-M. Magnan, J. Marrouche, B. Mathias, R. Nandi, J. Nash, A. Nikitenko⁴⁰, J. Pela, M. Pesaresi, K. Petridis, M. Pioppi⁵⁴, D.M. Raymond, S. Rogerson, A. Rose, C. Seez, P. Sharp[†], A. Sparrow, A. Tapper, M. Vazquez Acosta, T. Virdee, S. Wakefield, N. Wardle

Brunel University, Uxbridge, United Kingdom

M. Chadwick, J.E. Cole, P.R. Hobson, A. Khan, P. Kyberd, D. Leggat, D. Leslie, W. Martin, I.D. Reid, P. Symonds, L. Teodorescu, M. Turner

Baylor University, Waco, USA

J. Dittmann, K. Hatakeyama, A. Kasmi, H. Liu, T. Scarborough

The University of Alabama, Tuscaloosa, USA

O. Charaf, S.I. Cooper, C. Henderson, P. Rumerio

Boston University, Boston, USA

A. Avetisyan, T. Bose, C. Fantasia, A. Heister, P. Lawson, D. Lazic, J. Rohlf, D. Sperka, J. St. John, L. Sulak

Brown University, Providence, USA

J. Alimena, S. Bhattacharya, G. Christopher, D. Cutts, Z. Demiragli, A. Ferapontov, A. Garabedian, U. Heintz, S. Jabeen, G. Kukartsev, E. Laird, G. Landsberg, M. Luk, M. Narain, M. Segala, T. Sinthuprasith, T. Speer

University of California, Davis, Davis, USA

R. Breedon, G. Breto, M. Calderon De La Barca Sanchez, S. Chauhan, M. Chertok, J. Conway, R. Conway, P.T. Cox, R. Erbacher, M. Gardner, R. Houtz, W. Ko, A. Kopecky, R. Lander, T. Miceli, D. Pellett, J. Pilot, F. Ricci-Tam, B. Rutherford, M. Searle, J. Smith, M. Squires, M. Tripathi, S. Wilbur, R. Yohay

University of California, Los Angeles, USA

V. Andreev, D. Cline, R. Cousins, S. Erhan, P. Everaerts, C. Farrell, M. Felcini, J. Hauser, M. Ignatenko, C. Jarvis, G. Rakness, P. Schlein[†], E. Takasugi, P. Traczyk, V. Valuev, M. Weber

University of California, Riverside, Riverside, USA

J. Babb, R. Clare, J. Ellison, J.W. Gary, G. Hanson, J. Heilman, P. Jandir, H. Liu, O.R. Long, A. Luthra, M. Malberti, H. Nguyen, A. Shrinivas, J. Sturdy, S. Sumowidagdo, R. Wilken, S. Wimpenny

University of California, San Diego, La Jolla, USA

W. Andrews, J.G. Branson, G.B. Cerati, S. Cittolin, D. Evans, A. Holzner, R. Kelley, M. Lebourgeois, J. Letts, I. Macneill, S. Padhi, C. Palmer, G. Petrucciani, M. Pieri, M. Sani, V. Sharma, S. Simon, E. Sudano, M. Tadel, Y. Tu, A. Vartak, S. Wasserbaech⁵⁵, F. Würthwein, A. Yagil, J. Yoo

University of California, Santa Barbara, Santa Barbara, USA

D. Barge, C. Campagnari, T. Danielson, K. Flowers, P. Geffert, C. George, F. Golf, J. Incandela, C. Justus, D. Kovalskyi, V. Krutelyov, S. Lowette, R. Magaña Villalba, N. Mccoll, V. Pavlunin, J. Richman, R. Rossin, D. Stuart, W. To, C. West

California Institute of Technology, Pasadena, USA

A. Apresyan, A. Bornheim, J. Bunn, Y. Chen, E. Di Marco, J. Duarte, D. Kcira, Y. Ma, A. Mott,

H.B. Newman, C. Pena, C. Rogan, M. Spiropulu, V. Timciuc, J. Veverka, R. Wilkinson, S. Xie, R.Y. Zhu

Carnegie Mellon University, Pittsburgh, USA

V. Azzolini, A. Calamba, R. Carroll, T. Ferguson, Y. Iiyama, D.W. Jang, Y.F. Liu, M. Paulini, J. Russ, H. Vogel, I. Vorobiev

University of Colorado at Boulder, Boulder, USA

J.P. Cumalat, B.R. Drell, W.T. Ford, A. Gaz, E. Luiggi Lopez, U. Nauenberg, J.G. Smith, K. Stenson, K.A. Ulmer, S.R. Wagner

Cornell University, Ithaca, USA

J. Alexander, A. Chatterjee, N. Eggert, L.K. Gibbons, W. Hopkins, A. Khukhunaishvili, B. Kreis, N. Mirman, G. Nicolas Kaufman, J.R. Patterson, A. Ryd, E. Salvati, W. Sun, W.D. Teo, J. Thom, J. Thompson, J. Tucker, Y. Weng, L. Winstrom, P. Wittich

Fairfield University, Fairfield, USA

D. Winn

Fermi National Accelerator Laboratory, Batavia, USA

S. Abdullin, M. Albrow, J. Anderson, G. Apollinari, L.A.T. Bauerdick, A. Beretvas, J. Berryhill, P.C. Bhat, K. Burkett, J.N. Butler, V. Chetluru, H.W.K. Cheung, F. Chlebana, S. Cihangir, V.D. Elvira, I. Fisk, J. Freeman, Y. Gao, E. Gottschalk, L. Gray, D. Green, O. Gutsche, D. Hare, R.M. Harris, J. Hirschauer, B. Hooberman, S. Jindariani, M. Johnson, U. Joshi, K. Kaadze, B. Klima, S. Kunori, S. Kwan, J. Linacre, D. Lincoln, R. Lipton, J. Lykken, K. Maeshima, J.M. Marraffino, V.I. Martinez Outschoorn, S. Maruyama, D. Mason, P. McBride, K. Mishra, S. Mrenna, Y. Musienko⁵⁶, C. Newman-Holmes, V. O'Dell, O. Prokofyev, N. Ratnikova, E. Sexton-Kennedy, S. Sharma, W.J. Spalding, L. Spiegel, L. Taylor, S. Tkaczyk, N.V. Tran, L. Uplegger, E.W. Vaandering, R. Vidal, J. Whitmore, W. Wu, F. Yang, J.C. Yun

University of Florida, Gainesville, USA

D. Acosta, P. Avery, D. Bourilkov, M. Chen, T. Cheng, S. Das, M. De Gruttola, G.P. Di Giovanni, D. Dobur, A. Drozdetskiy, R.D. Field, M. Fisher, Y. Fu, I.K. Furic, J. Hugon, B. Kim, J. Konigsberg, A. Korytov, A. Kropivnitskaya, T. Kypreos, J.F. Low, K. Matchev, P. Milenovic⁵⁷, G. Mitselmakher, L. Muniz, R. Remington, A. Rinkevicius, N. Skhirtladze, M. Snowball, J. Yelton, M. Zakaria

Florida International University, Miami, USA

V. Gaultney, S. Hewamanage, S. Linn, P. Markowitz, G. Martinez, J.L. Rodriguez

Florida State University, Tallahassee, USA

T. Adams, A. Askew, J. Bochenek, J. Chen, B. Diamond, S.V. Gleyzer, J. Haas, S. Hagopian, V. Hagopian, K.F. Johnson, H. Prosper, V. Veeraraghavan, M. Weinberg

Florida Institute of Technology, Melbourne, USA

M.M. Baarmand, B. Dorney, M. Hohlmann, H. Kalakhety, F. Yumiceva

University of Illinois at Chicago (UIC), Chicago, USA

M.R. Adams, L. Apanasevich, V.E. Bazterra, R.R. Betts, I. Bucinskaite, J. Callner, R. Cavanaugh, O. Evdokimov, L. Gauthier, C.E. Gerber, D.J. Hofman, S. Khalatyan, P. Kurt, F. Lacroix, D.H. Moon, C. O'Brien, C. Silkworth, D. Strom, P. Turner, N. Varelas

The University of Iowa, Iowa City, USA

U. Akgun, E.A. Albayrak⁵¹, B. Bilki⁵⁸, W. Clarida, K. Dilsiz, F. Duru, S. Griffiths, J.-P. Merlo,

H. Mermerkaya⁵⁹, A. Mestvirishvili, A. Moeller, J. Nachtman, C.R. Newsom, H. Ogul, Y. Onel, F. Ozok⁵¹, S. Sen, P. Tan, E. Tiras, J. Wetzel, T. Yetkin⁶⁰, K. Yi

Johns Hopkins University, Baltimore, USA

B.A. Barnett, B. Blumenfeld, S. Bolognesi, G. Giurgiu, A.V. Gritsan, G. Hu, P. Maksimovic, C. Martin, M. Swartz, A. Whitbeck

The University of Kansas, Lawrence, USA

P. Baringer, A. Bean, G. Benelli, R.P. Kenny III, M. Murray, D. Noonan, S. Sanders, R. Stringer, J.S. Wood

Kansas State University, Manhattan, USA

A.F. Barfuss, I. Chakaberia, A. Ivanov, S. Khalil, M. Makouski, Y. Maravin, L.K. Saini, S. Shrestha, I. Svintradze

Lawrence Livermore National Laboratory, Livermore, USA

J. Gronberg, D. Lange, F. Rebassoo, D. Wright

University of Maryland, College Park, USA

A. Baden, B. Calvert, S.C. Eno, J.A. Gomez, N.J. Hadley, R.G. Kellogg, T. Kolberg, Y. Lu, M. Marionneau, A.C. Mignerey, K. Pedro, A. Peterman, A. Skuja, J. Temple, M.B. Tonjes, S.C. Tonwar

Massachusetts Institute of Technology, Cambridge, USA

A. Apyan, G. Bauer, W. Busza, I.A. Cali, M. Chan, L. Di Matteo, V. Dutta, G. Gomez Ceballos, M. Goncharov, D. Gulhan, Y. Kim, M. Klute, Y.S. Lai, A. Levin, P.D. Luckey, T. Ma, S. Nahn, C. Paus, D. Ralph, C. Roland, G. Roland, G.S.F. Stephans, F. Stöckli, K. Sumorok, D. Velicanu, R. Wolf, B. Wyslouch, M. Yang, Y. Yilmaz, A.S. Yoon, M. Zanetti, V. Zhukova

University of Minnesota, Minneapolis, USA

B. Dahmes, A. De Benedetti, G. Franzoni, A. Gude, J. Haupt, S.C. Kao, K. Klapoetke, Y. Kubota, J. Mans, N. Pastika, R. Rusack, M. Sasseville, A. Singovsky, N. Tambe, J. Turkewitz

University of Mississippi, Oxford, USA

J.G. Acosta, L.M. Cremaldi, R. Kroeger, S. Oliveros, L. Perera, R. Rahmat, D.A. Sanders, D. Summers

University of Nebraska-Lincoln, Lincoln, USA

E. Avdeeva, K. Bloom, S. Bose, D.R. Claes, A. Dominguez, M. Eads, R. Gonzalez Suarez, J. Keller, I. Kravchenko, J. Lazo-Flores, S. Malik, F. Meier, G.R. Snow

State University of New York at Buffalo, Buffalo, USA

J. Dolen, A. Godshalk, I. Iashvili, S. Jain, A. Kharchilava, A. Kumar, S. Rappoccio, Z. Wan

Northeastern University, Boston, USA

G. Alverson, E. Barberis, D. Baumgartel, M. Chasco, J. Haley, A. Massironi, D. Nash, T. Orimoto, D. Trocino, D. Wood, J. Zhang

Northwestern University, Evanston, USA

A. Anastassov, K.A. Hahn, A. Kubik, L. Lusito, N. Mucia, N. Odell, B. Pollack, A. Pozdnyakov, M. Schmitt, S. Stoynev, K. Sung, M. Velasco, S. Won

University of Notre Dame, Notre Dame, USA

D. Berry, A. Brinkerhoff, K.M. Chan, M. Hildreth, C. Jessop, D.J. Karmgard, J. Kolb, K. Lannon, W. Luo, S. Lynch, N. Marinelli, D.M. Morse, T. Pearson, M. Planer, R. Ruchti, J. Slaunwhite, N. Valls, M. Wayne, M. Wolf

The Ohio State University, Columbus, USA

L. Antonelli, B. Bylsma, L.S. Durkin, C. Hill, R. Hughes, K. Kotov, T.Y. Ling, D. Puigh, M. Rodenburg, G. Smith, C. Vuosalo, B.L. Winer, H. Wolfe

Princeton University, Princeton, USA

E. Berry, P. Elmer, V. Halyo, P. Hebda, J. Hegeman, A. Hunt, P. Jindal, S.A. Koay, P. Lujan, D. Marlow, T. Medvedeva, M. Mooney, J. Olsen, P. Piroué, X. Quan, A. Raval, H. Saka, D. Stickland, C. Tully, J.S. Werner, S.C. Zenz, A. Zuranski

University of Puerto Rico, Mayaguez, USA

E. Brownson, A. Lopez, H. Mendez, J.E. Ramirez Vargas

Purdue University, West Lafayette, USA

E. Alagoz, D. Benedetti, G. Bolla, D. Bortoletto, M. De Mattia, A. Everett, Z. Hu, M. Jones, K. Jung, O. Koybasi, M. Kress, N. Leonardo, D. Lopes Pegna, V. Maroussov, P. Merkel, D.H. Miller, N. Neumeister, I. Shipsey, D. Silvers, A. Svyatkovskiy, M. Vidal Marono, F. Wang, W. Xie, L. Xu, H.D. Yoo, J. Zablocki, Y. Zheng

Purdue University Calumet, Hammond, USA

N. Parashar

Rice University, Houston, USA

A. Adair, B. Akgun, K.M. Ecklund, F.J.M. Geurts, W. Li, B. Michlin, B.P. Padley, R. Redjimi, J. Roberts, J. Zabel

University of Rochester, Rochester, USA

B. Betchart, A. Bodek, R. Covarelli, P. de Barbaro, R. Demina, Y. Eshaq, T. Ferbel, A. Garcia-Bellido, P. Goldenzweig, J. Han, A. Harel, D.C. Miner, G. Petrillo, D. Vishnevskiy, M. Zielinski

The Rockefeller University, New York, USA

A. Bhatti, R. Ciesielski, L. Demortier, K. Goulios, G. Lungu, S. Malik, C. Mesropian

Rutgers, The State University of New Jersey, Piscataway, USA

S. Arora, A. Barker, J.P. Chou, C. Contreras-Campana, E. Contreras-Campana, D. Duggan, D. Ferencek, Y. Gershtein, R. Gray, E. Halkiadakis, D. Hidas, A. Lath, S. Panwalkar, M. Park, R. Patel, V. Rekovic, J. Robles, S. Salur, S. Schnetzer, C. Seitz, S. Somalwar, R. Stone, S. Thomas, P. Thomassen, M. Walker

University of Tennessee, Knoxville, USA

G. Cerizza, M. Hollingsworth, K. Rose, S. Spanier, Z.C. Yang, A. York

Texas A&M University, College Station, USA

O. Bouhali⁶¹, R. Eusebi, W. Flanagan, J. Gilmore, T. Kamon⁶², V. Khotilovich, R. Montalvo, I. Osipenkov, Y. Pakhotin, A. Perloff, J. Roe, A. Safonov, T. Sakuma, I. Suarez, A. Tatarinov, D. Toback

Texas Tech University, Lubbock, USA

N. Akchurin, C. Cowden, J. Damgov, C. Dragoiu, P.R. Duderu, K. Kovitangoon, S.W. Lee, T. Libeiro, I. Volobouev

Vanderbilt University, Nashville, USA

E. Appelt, A.G. Delannoy, S. Greene, A. Gurrola, W. Johns, C. Maguire, Y. Mao, A. Melo, M. Sharma, P. Sheldon, B. Snook, S. Tuo, J. Velkovska

University of Virginia, Charlottesville, USA

M.W. Arenton, S. Boutle, B. Cox, B. Francis, J. Goodell, R. Hirosky, A. Ledovskoy, C. Lin, C. Neu, J. Wood

Wayne State University, Detroit, USA

S. Gollapinni, R. Harr, P.E. Karchin, C. Kottachchi Kankanamge Don, P. Lamichhane, A. Sakharov

University of Wisconsin, Madison, USA

D.A. Belknap, L. Borrello, D. Carlsmith, M. Cepeda, S. Dasu, S. Duric, E. Friis, M. Grothe, R. Hall-Wilton, M. Herndon, A. Hervé, P. Klabbers, J. Klukas, A. Lanaro, R. Loveless, A. Mohapatra, M.U. Mozer, I. Ojalvo, T. Perry, G.A. Pierro, G. Polese, I. Ross, T. Sarangi, A. Savin, W.H. Smith, J. Swanson

†: Deceased

- 1: Also at Vienna University of Technology, Vienna, Austria
- 2: Also at CERN, European Organization for Nuclear Research, Geneva, Switzerland
- 3: Also at Institut Pluridisciplinaire Hubert Curien, Université de Strasbourg, Université de Haute Alsace Mulhouse, CNRS/IN2P3, Strasbourg, France
- 4: Also at National Institute of Chemical Physics and Biophysics, Tallinn, Estonia
- 5: Also at Skobeltsyn Institute of Nuclear Physics, Lomonosov Moscow State University, Moscow, Russia
- 6: Also at Universidade Estadual de Campinas, Campinas, Brazil
- 7: Also at California Institute of Technology, Pasadena, USA
- 8: Also at Laboratoire Leprince-Ringuet, Ecole Polytechnique, IN2P3-CNRS, Palaiseau, France
- 9: Also at Suez Canal University, Suez, Egypt
- 10: Also at Zewail City of Science and Technology, Zewail, Egypt
- 11: Also at Cairo University, Cairo, Egypt
- 12: Also at Fayoum University, El-Fayoum, Egypt
- 13: Also at British University in Egypt, Cairo, Egypt
- 14: Now at Ain Shams University, Cairo, Egypt
- 15: Also at National Centre for Nuclear Research, Swierk, Poland
- 16: Also at Université de Haute Alsace, Mulhouse, France
- 17: Also at Joint Institute for Nuclear Research, Dubna, Russia
- 18: Also at Brandenburg University of Technology, Cottbus, Germany
- 19: Also at The University of Kansas, Lawrence, USA
- 20: Also at Institute of Nuclear Research ATOMKI, Debrecen, Hungary
- 21: Also at Eötvös Loránd University, Budapest, Hungary
- 22: Also at Tata Institute of Fundamental Research - EHEP, Mumbai, India
- 23: Also at Tata Institute of Fundamental Research - HECR, Mumbai, India
- 24: Now at King Abdulaziz University, Jeddah, Saudi Arabia
- 25: Also at University of Visva-Bharati, Santiniketan, India
- 26: Also at University of Ruhuna, Matara, Sri Lanka
- 27: Also at Isfahan University of Technology, Isfahan, Iran
- 28: Also at Sharif University of Technology, Tehran, Iran
- 29: Also at Plasma Physics Research Center, Science and Research Branch, Islamic Azad University, Tehran, Iran
- 30: Also at Laboratori Nazionali di Legnaro dell' INFN, Legnaro, Italy
- 31: Also at Università degli Studi di Siena, Siena, Italy
- 32: Also at Purdue University, West Lafayette, USA
- 33: Also at Universidad Michoacana de San Nicolas de Hidalgo, Morelia, Mexico

-
- 34: Also at Faculty of Physics, University of Belgrade, Belgrade, Serbia
 - 35: Also at Facoltà Ingegneria, Università di Roma, Roma, Italy
 - 36: Also at Scuola Normale e Sezione dell'INFN, Pisa, Italy
 - 37: Also at University of Athens, Athens, Greece
 - 38: Also at Rutherford Appleton Laboratory, Didcot, United Kingdom
 - 39: Also at Paul Scherrer Institut, Villigen, Switzerland
 - 40: Also at Institute for Theoretical and Experimental Physics, Moscow, Russia
 - 41: Also at Albert Einstein Center for Fundamental Physics, Bern, Switzerland
 - 42: Also at Gaziosmanpasa University, Tokat, Turkey
 - 43: Also at Adiyaman University, Adiyaman, Turkey
 - 44: Also at Cag University, Mersin, Turkey
 - 45: Also at Mersin University, Mersin, Turkey
 - 46: Also at Izmir Institute of Technology, Izmir, Turkey
 - 47: Also at Ozyegin University, Istanbul, Turkey
 - 48: Also at Kafkas University, Kars, Turkey
 - 49: Also at Suleyman Demirel University, Isparta, Turkey
 - 50: Also at Ege University, Izmir, Turkey
 - 51: Also at Mimar Sinan University, Istanbul, Istanbul, Turkey
 - 52: Also at Kahramanmaras Sütcü Imam University, Kahramanmaras, Turkey
 - 53: Also at School of Physics and Astronomy, University of Southampton, Southampton, United Kingdom
 - 54: Also at INFN Sezione di Perugia; Università di Perugia, Perugia, Italy
 - 55: Also at Utah Valley University, Orem, USA
 - 56: Also at Institute for Nuclear Research, Moscow, Russia
 - 57: Also at University of Belgrade, Faculty of Physics and Vinca Institute of Nuclear Sciences, Belgrade, Serbia
 - 58: Also at Argonne National Laboratory, Argonne, USA
 - 59: Also at Erzincan University, Erzincan, Turkey
 - 60: Also at Yildiz Technical University, Istanbul, Turkey
 - 61: Also at Texas A&M University at Qatar, Doha, Qatar
 - 62: Also at Kyungpook National University, Daegu, Korea